

2

AD-A233 424

FTD-ID(RS)T-0356-00

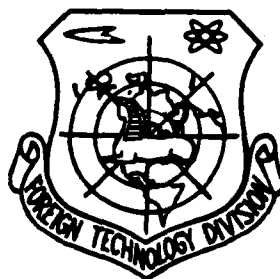
FOREIGN TECHNOLOGY DIVISION



NONDESTRUCTIVE TESTING
(Selected Articles)

DTIC

APR 11 1991



Approved for public release;
Distribution unlimited.



91 4 . 09 081

HUMAN TRANSLATION

FTD-ID(RS)T-0356-90

19 March 1991

MICROFICHE NR: FTD-91-C-000262

NONDESTRUCTIVE TESTING (Selected Articles)

English pages: 100

Source: Wusun Jiance, Vol. 11, Nr. 5, 1989,
pp. Title Page; 121-147

Country of origin: China

Translated by: Leo Kanner Associates
F33657-88-D-2188

Requester: FTD/TTTAV/Robert M. Dunco

Approved for public release; Distribution unlimited.

SEARCHED	INDEXED
SERIALIZED	FILED
MAR 21 1991	
FBI - WASHINGTON	
A1	

THIS TRANSLATION IS A RENDITION OF THE ORIGINAL FOREIGN TEXT WITHOUT ANY ANALYTICAL OR EDITORIAL COMMENT. STATEMENTS OR THEORIES ADVOCATED OR IMPLIED ARE THOSE OF THE SOURCE AND DO NOT NECESSARILY REFLECT THE POSITION OR OPINION OF THE FOREIGN TECHNOLOGY DIVISION.

PREPARED BY:

TRANSLATION DIVISION
FOREIGN TECHNOLOGY DIVISION
WPAFB, OHIO

TABLE OF CONTENTS

Graphics Disclaimer	11
Effect of Compensation on Ultrasonic Inspection of Pipe Welds, by Ji Liang, Yuan Rulong	1
English-Chinese Dictionary of Nondestructive Testing Terms	11
Control of K Value for Radiographic Inspection of Welded Joints, by Li Yan	12
Identification and Investigation of Incomplete Fusion of Welds on Radiographs, by Xin Zhongren, Ma Mingqiu, Xin Zhongzhi, Yang Jinjian ...	36
New Method of Nondestructive Testing of Internal Stresses--Magnetic Acoustic Emission, by Xu Yuehuang, Du Fengmu, Shen Gongtian	52
Analysis of Abnormal Defects on X-Ray Films, by Li Lanrui, Li Tongchao..	67
Measurement and Location of Welds for Radiographic Inspection, by Sun Wenhai	69
Discussion on Film Assessment of Weld Roots in Pad Welding, by Ren Shiping	71
Rules for Qualification and Certification of Nondestructive Test Personnel--Chinese People's Republic State Standard GB 9445-88	74
Models SD-I and SDIA Iridium ¹⁹² Gamma-Ray Flaw Detecting Machine	98

GRAPHICS DISCLAIMER

All figures, graphics, tables, equations, etc. merged into this translation were extracted from the best quality copy available.

EFFECT OF COMPENSATION ON ULTRASONIC INSPECTION OF PIPE WELDS

Ji Liang, Electric Construction Research Institute, Ministry of Electric Power and Resources; and Yuan Rulong, Second Engineering Company of Electric Construction, Anhui

The effect of compensation on ultrasonic flaw detection is studied with the practical examples of ultrasonic inspection of welds in the main steam pipes in a high-temperature, high-pressure power plant. Rules are found through tests.

Introduction

At a construction site of a 600MW prime mover generator set, in ultrasonic flaw detection of weld seams on large-diameter, thick-walled pipelines the authors discovered that an out-of-standard flaw was discovered at a site by using a Q search unit (2.5P17x17K1); the wave amplitude exceeds the scrapping line by 3dB (with compensation, 4dB). Upon rechecking, another R search unit (2.5P14x16K1) was employed; as a result, the amplitude of the echo wave of the flaw was lower than the corresponding scrapping line (with the same compensation, 4dB) by 2 to 3dB of the search unit. With step-by-step analysis of the flaw detection procedure, it was concluded that determining the value of compensation is the main factor leading to this discrepancy. Since there are numerous structural models of the examined components with different specifications, it is not possible to process each flaw detection object with the corresponding

reference block of measurement compensation. During flaw detection, values are often estimated by flaw detection personnel by drawing on their experience, so relatively large errors exist. To verify the above-mentioned analysis, the authors conducted the following experiments.

Measurement of Value of Compensation

With on-site flaw detection of the main steam pipes (OD673x103mm), a special reference block (Fig. 1) for measuring the compensation value was machined; the reference block is referred to as the PB reference block.

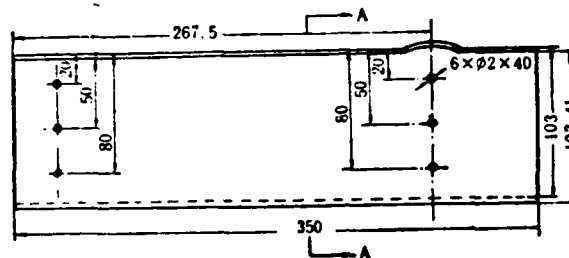


Fig. 1. Dimensions and shape of PB reference block

Remark: Material property - SA-335-P22
Scale - 2:1 Unit - mm

To correspond as closely as possible to the actual test conditions, the reference block was machined with a section of sampled main steam pipe containing a weld seam; its surface conditions and heat treatment technique were the same as for other main steam pipe with respect to engineering. In addition, the following conditions were set in the experiment:

Instrument: model CTS-22 ultrasonic flaw detection instrument made at Shantou;

Search unit: 2.5P, K1 angled search unit;

Determination of wave amplitude: for a certain gain, the

wave amplitude was adjusted to the readout dB of the attenuator at 80% of full graduation of the fluorescence; and

Standard reference block: model SD-II standard reference block (Fig. 2). The shape and dimensions of the above-mentioned reference block are somewhat different from those of SD-II reference block specified in SDJ-67-83 standard. The experimental results with the two reference blocks are in agreement.

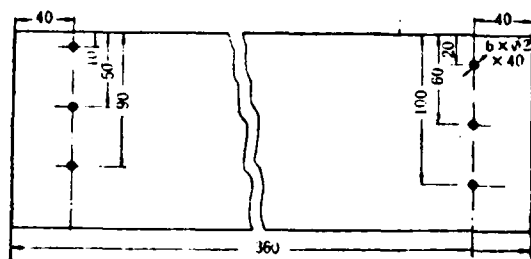


Fig. 2. SD-II reference block
Remark: Material property - SA-335-P22
Unit in the diagram - mm

Before the use of a new coupling plan as the plan for the search unit, the distance versus wave amplitude curve of the search unit should be plotted by using an SD-II reference block and a certain calibration sensitivity ($R_{40}=qdB$). Then the PB reference block was used to measure the difference of the echo wave amplitude of the same reflector with the corresponding depth. This is what is generally referred to as the compensation value. However, after the search unit was used for a certain period of time, the contact surface becomes a concave surface. At that time, the distance versus wave amplitude curve is then measured on the SD-II reference block; then the difference value obtained is compared with that of the PB reference block. The authors designated this value as the dynamic compensation value, which is listed in Table 1 as the experimental index. In Table 1, the plus and minus symbols in front of the absolute values in

the column of the dynamic compensation value represent, respectively, the positive and the negative values of the compensation value. The plus or minus symbols at the right upper corner of the absolute value figure signify that the value is slightly higher or slightly lower than the figure thus expressed. For example, 6^+ is slightly higher than 6; and 6^- is slightly lower than 6.

Analysis of Experimental Results

The following conclusions can be obtained from Table 1:

1. For unworn new search units (numbers 1 through 6 experimental search units), the data listed in the column headed with Dynamic compensation value are the compensation values actually required. From the data in the table, these values are very small, with the largest not exceeding 2dB; this shows why only very small compensations (approximately 1-2dB) are required, or even no compensation. The value is expressed as OA in Fig. 3.

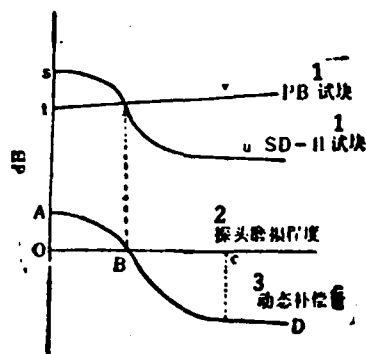


Fig. 3. Schematic diagram for dynamic compensation value
KEY: 1 - Reference block 2 - Degree of search unit wear
3 - Dynamic compensation value

TABLE 1. Experimental Data

1 序号	晶片尺寸 2 和探头编号 (mm)	$\phi 2 \times 40$ ³ mm 人工反射 体深度	$\phi 2 \times 40$ mm人工 ⁴ 反射体波幅		6 动态 补偿量
			SD-1 试块 5	PB试块 5	
1	10×12 A*	50	48	48	0
		80	41	41 ⁺	-10 ⁺
2	10×12 C* (磨损前) 7	50	49	50 ⁻	-11 ⁻
		80	42	42 ⁺	-0 ⁺
3	14×16 B*	50	51 ⁻	53	+11 ⁻
		80	47	45	+12 ⁻
4	14×16 E*	50	47	46	+11 ⁻
		80	40 ⁺	39 ⁺	+11 ⁻
5	17×17 P*	50	49	49	0
		80	44	44 ⁺	-10 ⁺
6	17×17 B*	50	52	51	+11 ⁻
		80	46 ⁺	45	+11 ⁺
7	10×12 B*	50	42 ⁺	48	-16 ⁻
		80	36	42	-16 ⁻
8	10×12 C* ⁸ (磨损后)	50	44	50	-16 ⁺
		80	37	44	-17 ⁻
9	10×12 D*	50	44 ⁻	50	-16 ⁺
		80	36 ⁺	44	-18 ⁻
10	17×17 C*	50	44 ⁻	50 ⁺	-17 ⁻
		80	39	49 ⁻	-19 ⁺
11	17×17 D*	50	44	50	-16 ⁻
		80	38	46	-18 ⁻

KEY: 1 - Sequence number 2 - Chip dimensions
and search unit number (mm) 3 - Depth of artificial
reflector 4 - Wave amplitude of artificial
reflector 5 - Reference block 6 - Dynamic
compensation 7 - Before grinding wear
8 - After grinding wear

2. After a certain amount of search unit wear (search unit numbers 7 through 11), from Fig. 3 the dynamic compensation value has reached or is approaching C as the value becomes negative. This indicates that the dynamic compensation value becomes gradually smaller with increasing grinding wear of the search unit. As shown in Table 1, the number one experiment shows the dynamic compensation value measured after grinding wear of the same search unit as in experiment number 2.

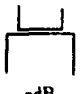


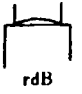
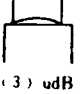
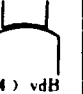
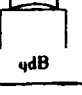

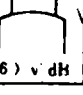
3. In experiments numbers 7 through 11, this indicates that the magnitude of the dynamic compensation value is related to the reflector depth. With increasing reflector depth from 50mm to 80mm, the dynamic compensation value is slightly reduced. As shown in experiment number 9, the dynamic compensation value measured with a 50mm deep reflector is $-|6^+|$; however, the dynamic compensation value measured with the 80mm reflector is $-|8^-|$. In other numbered experiments, this phenomenon also exists to differing degrees. However, this phenomenon is not clearly manifested when the search unit is not worn through grinding.

4. Table 2* is a table for analyzing the deviation of the compensation values. State 1 indicates the initial state of the search unit prior to grinding wear. By using the calibration sensitivity of $R40=qdB$, the distance versus wave amplitude wave curve is plotted on an SD-II reference block; therefore, the dynamic compensation value $(s-t)dB$ measured in this state is the compensation value actually required. However, in daily flaw detection practice no PB reference block is used in measuring the compensation value; generally, flaw detection personnel estimate the compensation values by relying on their experience. Assume that the estimated value is 4dB, the absolute value

*In Table 2, all errors of compensation values are absolute values.

$|4-(s-t)|$ dB of the difference of the compensation value actually required is the deviation in this state. From the experimental results in numbered experiments 1 through 6 in Table 1, $(s-t)$ falls within the range of 0 to 2dB; therefore, $|4-(s-t)|$ is 2 to 4dB.

TABLE 2. Table for Analysis of Deviation in Compensation Values

1 状态 编号	2 R40校准 灵敏度	3 SD-II 试块 试验结果	4 PB试块 试验结果	5 动态补偿量	6 人为所加 补偿量	7 实际所加 补偿量	8 实际所需 补偿量	9 补偿量误差
1	 qdB	 (1) sdB	 (2) tdB	$(S-t)$ dB	4dB	4dB	$(S-t)$ dB	$4-(S-t)$ dB
2	 rdB	 (3) udB	 (4) vdB	$(u-v)$ dB	4dB	4dB	$(S-v)$ dB	$4-(S-v)$ dB
3	 qdB	 (5) u dB	 (6) v' dB	$(u'-v')$ dB	4dB	$[4+(q-r)]$ dB	$(S-v)$ dB	$4+(q-r)$ $-(S-v)$ dB

KEY: 1 - Number of state 2 - Calibration sensitivity
 3 - Experimental results with SD-II reference block
 4 - Experimental results with PB reference block
 5 - Dynamic compensation values 6 - Artificially
 applied compensation values 7 - Actually applied
 compensation values 8 - Actually required compen-
 sation values 9 - Errors of compensation values

Conditions of the instrument in state 2 are the same as those in state 1; that is, the gain knob is not moved. Since the search unit has a certain amount of grinding wear, the contact surface is ground into a concave surface; the wave amplitude on the calibrated reference block R40 is reduced from the original qdB to rdB; the echo wave height of the reflector with prescribed depth on an SD-II reference block also decreases to udB from the original sdB. Since the distance versus wave amplitude curve is not plotted in this state, the dynamic compensation value $(u-v)$ dB measured at that time cannot represent the actually

required compensation value, which should be the difference between the data point s dB on the distance versus wave amplitude curve and v dB, the wave amplitude of a reflector with the same depth on a PB reference block for the search unit in this state: $(s-v)$ dB. Assume that the artificial compensation value has not been revised in time and is still 4dB; then the absolute value $|4-(s-v)|$ dB of the difference between the two indicates the deviation of the compensation value in that state. Since $v > t$, $|4-(s-v)| > |4-(s-t)|$. According to Table 1, the value of $|4-(s-v)|$ is known to reach a value as high as 5 to 6dB.

After grinding wear of the search unit, the wave amplitude may decrease to r dB from the original q dB when calibrated with an R40 reference block; at that time, the wave height restored to the q dB through the gain knob by the flaw detection personnel because they considered that the distance versus wave amplitude curve can be used only in the situation $R40=q$ dB, thus forming state 3 in the table. This calibration procedure raised sensitivity by $(q-r)$ dB; the reflector wave amplitude on the PB reference block (corresponding to the actual workpiece) will not be reduced because of the concave surface on the search unit. Conversely the original t dB becomes v dB because of better coupling. On adding 4dB of the artificial compensation, the actually added compensation value is $[4+(q-r)]$ dB. Then, can $(s-v')$ be used to indicate directly the required compensation value? Since the instrument state expressed by state 3 is not the same as state 1; only in the situation of the same instrument state can these two be deducted directly in order to obtain the compensation value. Therefore $(s-v')$ cannot represent the actually required compensation value in state 3. Since the instrument state of state 2 is the same as that of state 1, and the search unit state is the same as state 3, the required compensation value $(s-v)$ in state 2 is the required compensation value in state 3. Thus, the obtained deviation of compensation value in state 3 is $|4+(q-r)-(s-v)|$ dB, which is actually the

summation of the three-deviation difference; the value is relatively appreciable.

From data in Table 1 and from Fig. 3, it is apparent that the echo wave amplitude does not increase appreciably although the coupling condition on the PB reference block is improved after wearing of the coupling surface of the search unit into a curved surface. This is because of the diffusion of sound beams in the coupling state of the curved state; refer to Fig. 4 for its principle.



Fig. 4. Schematic diagram of sound beams scattered by the curved surface of the coupling search unit
KEY: 1 - Organic glass 2 - Steel

Discussion

The above-mentioned discussion explains that measurements should be made of the compensation value before a search unit is used, and the original data should be provided for calculating the search unit compensation value after grinding wear. A certain deviation exists in artificial estimates; for instance, in the example mentioned at the beginning of this article, the artificial estimate is 4dB, but the actually required compensation value is only between 0 and 2dB.

Both Table 1 and Fig. 3 sufficiently explain that the compensation value becomes smaller with steady deepening of the extent of search unit grinding wear. When a certain amount of

grinding wear is attained, both the dynamic compensation value and the compensation value reach minima after passing through point C as shown in Fig. 3. This value does not vary with continual grinding wear of the search unit.

To eliminate the deviation of the (q-r) item in state 3, effective measures should be taken to ensure the instrument state (primarily as the gain) to maintain constancy throughout the flaw detection procedure and during the next flaw detection session. Only by ensuring this point can no calibration be required for sensitivity by using R40 reference blocks. In the grinding wear process of flaw detection for a Q search unit at the beginning of this article, engineering personnel steadily calibrate by using R40 reference blocks, so the deviation of the (q-r)-th order exists; this is equivalent to determining the flaw to a higher value by $[4+(q-r)-(s-v)]\text{dB}$. According to preliminary experiments, (q-r) may reach a value in the vicinity of 5dB.

The authors are grateful for assistance given in the experiments by the relevant departments of the Second Engineering Company of Electric Construction, Anhui.

REFERENCES

1. Technical Norms of Construction and Acceptance of Power Generation Projects (Part of Ultrasonic Inspection of Pipe Welds), SDJ 67-83, Water Conservation and Power Generation House, 1984, 1, 13.
2. Chaoshengbo Tanshang [Ultrasonic Flaw Detection], Power Generation Industry Publishing House, 1980, 11.
3. Chaoshengbo Tanshang Fa [Ultrasonic Method of Flaw Detection], Gwangdung Publishing House of Science and Technology, 1981, 6.

YINGHAN WUSUN JIANCE CIHUI [English-Chinese Dictionary of
Nondestructive Testing Terms]

As a reference book, this dictionary is a collection of about 18,000 terms and abbreviations; most of the terms are basic terms and special terms frequently used in English books and journals on nondestructive testing. The technical terms are in the following fields: ultrasonics, rays, electromagnetism, eddy current, permeability, sound emission, stress, laser, infrared rays, and microwaves, among other fields. In addition, the dictionary also includes technical terms related to the following professions involved in the nondestructive testing specialty: physics, electronics, computer science, machines, and metallurgy, among others. This dictionary was compiled by the Nondestructive Testing Institute of the China Society of Mechanical Engineering; the dictionary can serve as a reference book for scientific researchers in the nondestructive testing specialty, and the field-related engineers, technicians, technical translators, as well as teachers and students of the corresponding universities and professional colleges. The dictionary was scheduled to be published in June 1989.

CONTROL OF K VALUE FOR RADIOGRAPHIC INSPECTION OF WELDED JOINTS

Li Yan, Wuxi Boiler Works

The author discusses the significance of controlling the penetrating thickness ratio K and the maximum thickness ratio K_{\max} in the radiographic inspection of welded joints, referring to the new national standard GB 3323-87 that has been published. Taking typical radiographic inspections as examples, the paper presents particular methods for controlling the K value and the K_{\max} value, as well as practical applications.

I. Introduction

In the newest revised international standard GB3323-87, "Radiography and Quality Classification of Butt Joints of Steel Melt Welding," control requirements on the thickness ratio K for radiographic inspection are mentioned. In similar standards abroad, such as BS 2600/I-73, ISO R1106-72, and JIS Z3104-74, similar requirements are also mentioned, only with different formulation approach. The requirements of the K value are listed in two international standards; this indicates that China's radiographic technique of flaw detection has been raised to a new quantitative level. However, a correct understanding is necessary for the meaning and control of the K value; otherwise, confusion or misdirection will be present in work practice.

II. Definition of the K Value

In radiography, the so-called penetration thickness ratio K is the ratio between the slant-direction penetration thickness and the terminal portion of the penetrating zone of the X-ray beam to the actual thickness of the terminal point. However, for weld seams generally K is the ratio between the thickness of the parent material penetrated in the slant direction at the terminal portion to the actual thickness of the parent material, or the ratio between the weld seam thickness slant-direction penetrated at the terminal portion to the actual weld seam thickness at the site. As shown in Figs. 1 and 2, whether the longitudinal or annular seams, the penetrating thickness ratio K^* can be represented by the following formulas:

$$K = \frac{AA'}{AG} = \frac{BB'}{BH} = \frac{T'}{T} \quad (1)$$

$$K = \frac{CC'}{CQ} = \frac{DD'}{DR} = \frac{T_A'}{T_A} \quad (2)$$

After it is certain that the light exposure conditions are satisfied for the blackness range requirements in the exposure zone, consideration should be given to the ratio between the weld seam thickness T_A' of slant-direction penetration, and the actual thickness T of the parent material; this ratio value is called the maximum thickness ratio K_{\max} , that is:

$$K_{\max} = \frac{T_A'}{T}$$

The following equations can be used for replacement in the relation between the difference ΔT (that is, $T' - T$) or ΔT_A (that is, $T_A' - T_A$) of the exposure thickness, and the exposure thickness ratio K :

*Based on the text of the standard, the definition of K should be Eq. (1), butt annular weld seam. Strictly speaking, $K_{\text{material}} \neq K_{\text{seam}}$. For sake of simplicity, however, it is acceptable for $K_{\text{material}} \approx K_{\text{seam}}$.

$$K = 1 + \frac{\Delta T}{T} = 1 + \frac{\Delta T_A}{T_A}$$

$$\Delta T = (K-1)T \quad \Delta T/T = K-1$$

$$\Delta T_A = (K-1)T_A \quad \Delta T_A/T_A = K-1$$

For example, $K=1.1$ and $K=1.06$ can be represented, respectively, by $\Delta T=10\%T$ (or $\Delta T/T=10\%$) and $\Delta T_A=10\%T_A$ (or $\Delta T_A/T_A=10\%$). Such representations are used in BS 2600/I and ISO R1106.

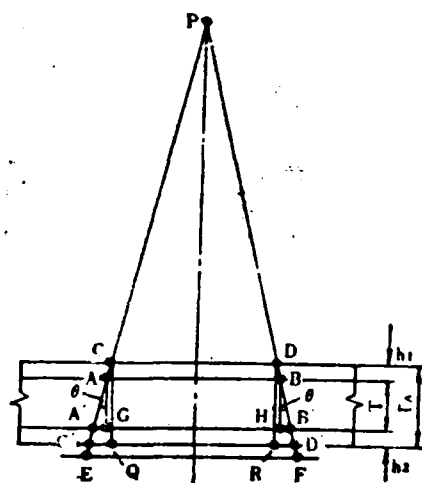


Fig. 1. Exposure thickness ratio K of longitudinal seam, and maximum exposure ratio K_{max}

Remarks: T - thickness of parent material T_A - thickness of weld seam h_1, h_2 - residual height \overline{AB} - single-exposure length L_3 \overline{EF} - effective assessment length L_{eff}
 $\overline{AA'} = \overline{BB'} = T' \quad \overline{CC'} = \overline{DD'} = T_A'$

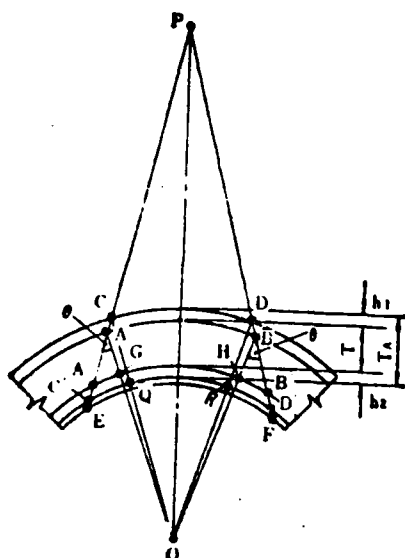


Fig. 2. Exposure thickness ratio K of longitudinal seam, and maximum exposure ratio K_{\max}
 Remarks: T - thickness of parent material T_A - thickness of weld seam h_1, h_2 - residual height \overline{AB} - single-exposure length L_3 \overline{EF} effective exposure length L_{eff}
 $\overline{AA'} = \overline{BB'} = T' \quad \overline{CC'} = \overline{DD'} = T_A'$

III. Practical Significance of Controlling the K Value

During exposure of steel weld seams, the practical significance of controlling the exposure thickness ratio K value is the following:

(1) The K value is so controlled that the exposure amount does not have too great a difference for X-rays arriving at the X-ray film in the center of the exposure zone after passing through two terminals of the weld seam; thus, varying of the negative blackness and the sensitivity of the image quality meter are controlled within a certain range.

(2) The K value is so controlled that the exposure angles of

the lateral-direction crack type defects along the wall thickness direction of two terminals of the exposure zone are not too much different, thus enhancing the detection rate of the hazardous defects like cracks.

It is known from fundamental experiments that, owing to the structure relationship of the X-ray tube, the distributions of optical focal lengths and X-ray intensities of industrial X-rays are different (as shown in Fig. 3) [4] in the entire exposure field composed in the conventional 40° conical angle. Generally, the focus dimensions of the anode side and the cathode side are 1:4. In other words, for two defects of the same size and depth positions, their geometric fuzziness on the negative may vary by four times if the two defects are placed at two terminals of the exposure field (the anode side and the cathode side).

It is apparent from Fig. 3 that there is an uneven property distribution of X-rays in the entire exposure field: when the half-exposure angles η are respectively, 20° , 13° , and 10° , the ratios of X-ray exposure intensities are, respectively, about 1:3, 1:1.5, and 1:1.3. Therefore, it is known that the negative blackness is apparently different for the anode side and the cathode side, even for the same exposure thickness because of obvious difference in intensity at both sides of the exposure field.

Fig. 4 shows the curve for a relation [4] of the X-ray exposure angle versus the crack detection rate deduced from exposure experiments on weld seam test plates. It is apparent from the figure that the distinguishing variation of cracks in the negative is not large for an exposure approximately less than 10° . When the exposure angle exceeds 15° , the crack detection rate apparently decreases with increase in exposure angle.

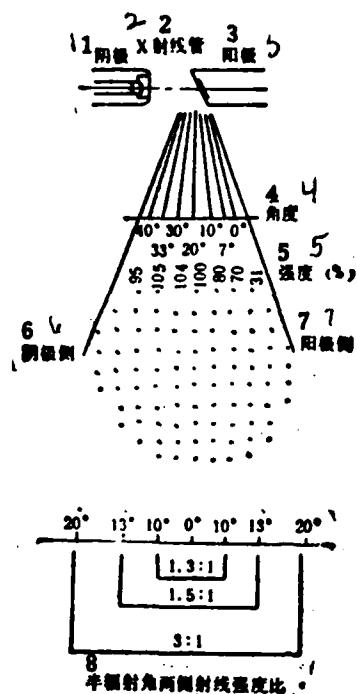


Fig. 3. Variations of intensity distribution, focus dimension, and shape within the X-ray exposure field

KEY: 1 - Cathode 2 - X-ray tube 3 - Anode
 4 - Angle 5 - Intensities 6 - Cathode side
 7 - Anode side 8 - Intensity ratios of X-rays
 at both sides of half-radiation angle

Therefore, the entire exposure field cannot be used for the exposure of a weld seam, but only for utilizing, as much as possible, the middle portion (that is, the range of $\eta = \pm 14^\circ$) of the exposure field for exposure. Physically, the control of the K value amounts to controlling the exposure ratio thickness; actually, this is the control of the dimension of the effective exposure field, the control of the ratio between the crack exposure angle and the X-ray intensity; therefore, this relates to the control of the effective exposure length required for sensitivity of the image quality meter in order to satisfy a certain degree of blackness.

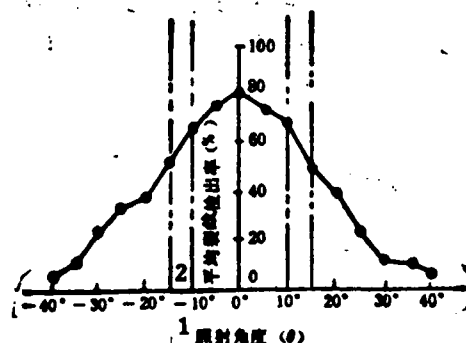


Fig. 4. Relation between exposure angle versus average crack detection rate
KEY: 1 - Exposure angle 2 - Average crack detection rate

During the exposure of a longitudinal seam based on the requirements of the photographic method of grades A, AB, and B (that is, $K=1.03$ and $K=1.01$) according to the specifications of GB 3323-87 Standard, the utilized effective half-radiation angle η are, respectively, 14° and 9.5° . However, during the exposure of an annular seam, also the requirements of the K value is realized (for grades A and AB, 1.1; and for grade B, 1.06), yet the utilized effective half-radiation η is smaller than that during the exposure of the longitudinal seam.

The maximum K value during X-ray photography of weld seams is directly related to control conditions of light exposure. For the corresponding minimum blackness and the maximum blackness corresponding to the maximum thickness T_A' and the minimum thickness T of the X-ray exposure on the radiographic negative within the blackness range stipulated in the standard, generally the light exposure conditions (tube voltage and the light exposure amount) as determined by the light exposure curve should allow the corresponding ratio of the light exposure amount of the maximum exposure thickness ratio not greater than the ratio of light exposure amount corresponding to the maximum difference of blackness allowed by the standard (refer to V for details).

IV. Single-Exposure Length Related to the K Value

When section by section light exposure is adopted for weld seams, the weld seam length exposed in each light exposure is called the single-exposure length L_3 , whose projection length onto the radiographic negative is called the effective assessment length L_{eff} . However, determination of L_3 should satisfy the requirements on exposure thickness ratio K . Therefore, there is a certain limiting relation between L_3 and the distance L_1 from the radiation source to the workpiece surface.

1. Requirements on the K value in longitudinal seam exposure and single-exposure length

The requirements on the K value originate from the requirements on lateral-direction crack detection angle (or the maximum distortion angle of the image) θ in the terminal portion of the exposure zone. To meet different requirements of the GB 3323-87 Standard on the longitudinal seam exposure thickness ratio K value to adapt to different grades of image quality, L_1 and L_3 should be determined from the following:

for grade A

for grade AB, when $L_1 \geq 2L_3$, $\theta \leq 14^\circ$, $K \leq 1.03$

for grade B, when $L_1 \geq 3L_3$, $\theta \leq 9.5^\circ$, $K \leq 1.01$

However, the single-exposure length L_3 on the workpiece surface is not equal to the effective assessment length L_{eff} on the negative. From Fig. 5, $L_{eff} = L_3 + \Delta L$; however, $\Delta L = (L^2 \cdot L_3) / L_1$.

When $L_1 = 2L_3$, $\Delta L = L_2 / 2$; and

When $L_1 = 3L_3$, $\Delta L = L_2 / 3$.

Here, ΔL is the lapping length of two adjacent negatives during exposure of a weld seam; this is the function of the

workpiece thickness.

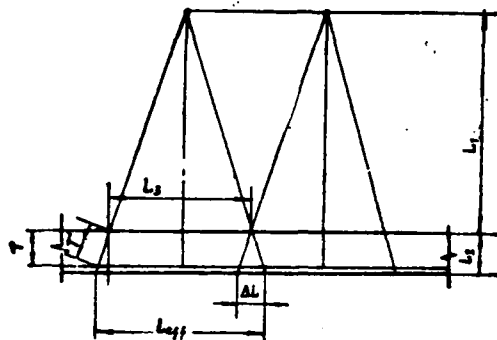


Fig. 5. Relation between L_3 and L_1 versus θ and K in longitudinal seam exposure method

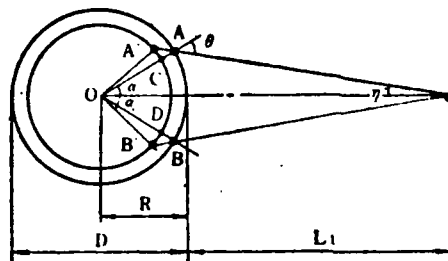
2. Requirements on the K value and single-exposure length in annular seam exposure

When exposure of an annular seam is carried out, generally the requirements on the K value in other exposure modes cannot be the same as those on the K value for butting a longitudinal seam besides the adoption of internal exposure center method by placing the radiation source at the position of the circle's center, or the internal exposure eccentric method with a radiation source not deviating far from the circle's center. Otherwise, the welding seam length will be very short for each exposure, and the working efficiency of radiography will be lowered. Therefore, the GB3323-87 Standard, the BS 2600 Standard, and the ISO R1106 Standard only impose requirements of 1.1 (ordinary grade and relatively higher grade) and 1.06 (high grade) for the K value on exposure of annular seams. In other words, control of the lateral-direction crack detection angle of annular weld seams, or image distortion angle will be relaxed to a certain extent than in the case of a longitudinal seam. In the following, a discussion is made on the external exposure method and the dual-wall single-image method, which are used as

examples; these methods are mostly used with the most representative feature.

a. External exposure method (the exposure method with the radiation source at the outside and the film inside)

To determine the single-exposure length L_3 of the annular seam, the minimum light exposure times N to satisfy the requirements of a certain K value for 100% exposure of the entire ring of an annular weld seam can be first determined, as shown in Fig. 6.



$$\widehat{AB}=L, \widehat{CD}=L', \widehat{A'B'}=L'', \overline{AA'}=T', \overline{AC}=T$$

Fig. 6. Determination of the single-exposure length L_3 at the radiation source site in the external exposure method for weld seams

$$N = \frac{180^\circ}{\alpha}$$

In this equation, $\alpha = \theta - \eta$.

In $\triangle OAA'$, we obtain the following from the theorem of cosines:

$$\begin{aligned} \cos \theta &= \frac{R^2 + T'^2 - r^2}{2RT'} \\ &= \frac{1}{K} \left[\frac{T(K^2 - 1)}{D} + 1 \right] \end{aligned}$$

$$\text{When } K=1.1, \theta = \cos^{-1} \frac{0.21T + D}{1.1D}$$

$$\text{When } K=1.06, \theta = \cos^{-1} \frac{0.12T + D}{1.06D}$$

η can be obtained from the theorem of sines:

$$\frac{\sin \eta}{R} = \frac{\sin (180^\circ - \theta)}{L_1 + R}$$

$$\therefore \eta = \sin^{-1} \left(\frac{D}{D + 2L_1} \cdot \sin \theta \right)$$

The single-exposure length L_3 at the radiation source site for the weld seam is:

$$L_3 = \frac{\pi D}{N}$$

In Fig. 7, the external exposure method is used for 100% exposure of an annular seam, and the relation between the minimum light exposure times, on the one hand, T/D and D/L_1 , on the other, when K is 1.1.

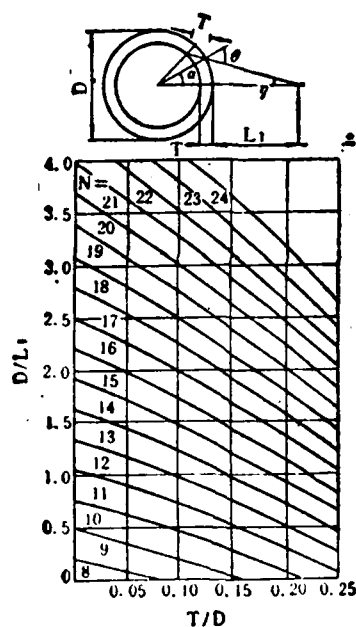


Fig. 7. Minimum light exposure times when $K=1.1$ when the annular seam external exposure method is used

b. Dual-wall single-image method

When the dual-wall single-image method of exposure is used for container or pipe annular seams, the following equation (refer to Fig. 8) is used to obtain the minimum light exposure

times when satisfying the requirements of a certain K value:

$$N = \frac{180^\circ}{\alpha}$$

In the equation, $\alpha = 0 + \eta$

$$\theta = \cos^{-1} \left\{ K^{-1} \left[\frac{T}{D} (K^2 - 1) + 1 \right] \right\}$$

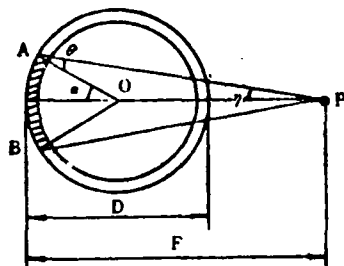
When $K=1.1$, $\theta = \cos^{-1} \frac{0.21T + D}{1.1D}$

When $K=1.06$, $\theta = \cos^{-1} \frac{0.12T + D}{1.06D}$

However,

$$\eta = \sin^{-1} \left(\frac{D}{2F - D} \cdot \sin \theta \right)$$

$$L_3' = \frac{\pi D}{N}$$



$$\widehat{AB} = L_3' = L_{3''}$$

Fig. 8. Determination of the minimum light exposure times N and the single-exposure length L_3' at the film site when dual-wall single-image method is used for annular seams

There are two limiting situations: when $F \rightarrow D$, and $T \ll D$, the effective range of exposure (the portion of slant lines in the figure) is the largest; however, when $F \rightarrow \infty$, the effective exposure range is minimum, that is,

$$\lim_{F \rightarrow D} \alpha = 2\theta$$

$$\lim_{F \rightarrow \infty} \alpha = \theta$$

In the dual-wall single-image method for annular seams, therefore, the minimum and maximum number of films photographed can be represented by the following equations:

$$N_{\min} = \frac{90^\circ}{\theta}$$

$$N_{\max} = \frac{180^\circ}{\theta}$$

If consideration is given to the fact that the exposure angle θ is 15° for lateral-direction cracks along the wall thickness direction at both terminals of the exposure zone, then

$$N_{\min} = \frac{90^\circ}{15^\circ} = 6$$

$$N_{\max} = \frac{180^\circ}{15^\circ} = 12$$

Fig. 9 shows the relation between the minimum light exposure times of weld seams when $K=1.1$, on the one hand, and T/D , D/E , and D/F , on the other hand, in various exposure methods. In the figure, only the condition $D/F \leq 1.0$ is given for the dual-wall single-image method. From the figure, when D/L_1 or D/F is constant when applying the external exposure method and the dual-wall single-wall exposure method, the number of photographic films that satisfy $K=1.1$ is gradually increased with increase in T/D by exceeding a certain range. In addition, the relative speed of increase in the number of photographic films in the external exposure method is relatively high. Besides, when T/D is a constant, the number of photographic films is increased under the external exposure method when the increase in D/L_1 exceeds a certain range; however, for the dual-wall single-image method, the number of photographic films is decreased if a certain range is exceeded when there is an increase in D/F .

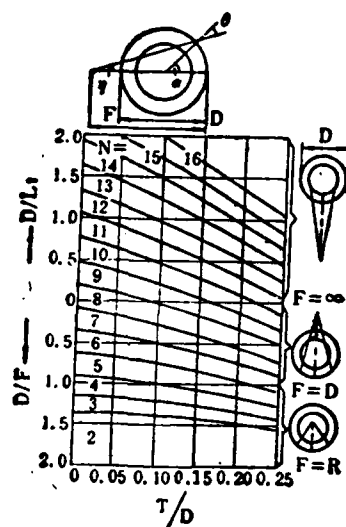


Fig. 9. Determination of the minimum light exposure times for annular seams when $K=1.1$ in the multiple-exposure method

V. Effect on Light Exposure Conditions of the Maximum K Value for the Maximum Difference in Thickness

1. The restraining relation of the maximum K value and light exposure conditions

For a weld seam with a level plate and ground level of the weld seam residual height, the exposure thickness is related not only to the detection angle for a lateral crack and the single-exposure length, but also is directly related to the revised conditions of light exposure. However, for weld seams with residual height, the maximum exposure thickness ratio K_{\max} should be a directly relevant factor in controlling the light exposure conditions.

In X-ray photography of weld seams, generally selection of

light exposure conditions should enable X-rays to fall within the negative exposure range; the blackness in the negative after penetrating with the maximum exposure thickness (both terminals are weld seams) and the minimum exposure thickness (the heat-affected zone in the vicinity of the center of the examined zone) fall within the range stipulated by the standard (such as the blackness range between 1.2 and 3.5 as specified in GB 3323-87). Moreover, it is required that the photographic sensitivity within the effective exposure range meets the specified index. Therefore, the maximum thickness ratio K_{\max} of exposure should be used to determine the tube voltage and light exposure meeting the requirements of negative blackness and sensitivity of the image quality meter. On this aspect, relatively satisfactory results can be realized by using the light exposure curve and film property curve plotted from a series of light exposure experiments.

Generally, it is customary to find the correct exposing light conditions from a figure of the light exposure curve for weld seam thickness at the exposure zone center; in so doing, frequently no negative quality meeting the requirements is realized. Therefore, the tube voltage and light exposure should be correctly selected based on the thickness ratio and the blackness in the exposure zone, sensitivity of light quality meter, and clarity.

Generally, technical terms of the maximum thickness difference are applied. Conversion can be carried out by using the following equations for the maximum thickness ratio K_{\max} and the maximum thickness difference ΔT_{\max} (refer to Figs. 1 and 2 for the meaning of the symbols in the equations):

$$\begin{aligned} K_{\max} &= \frac{T_A'}{T} & \Delta T_{\max} &= T_A' - T \\ \text{Or,} & & \Delta T_{\max} &= (K_{\max} - 1)T \end{aligned}$$

2. Maximum thickness difference and the feasible tube voltage

In principle, the tube voltage should be so selected for exposure of welded joints with given thickness difference of exposure, the ratio of light exposure (ψ') of the film after the X-rays penetrate the minimum thickness and the maximum thickness within the effective range is not greater than the ratio (ψ) [1, 2] of the corresponding light exposure in the stipulated range of blackness obtained when using the film.

As shown in Fig. 10, if the stipulated range of blackness is D_1 and D_2 , and the condition of blackness of the light exposure curve is D_1 , then for a weld seam with thickness T for the exposure plate and T_A equal to the plate thickness adding the residual height, then

$$\frac{E_2'}{E_1'} = \psi' > \frac{E_2}{E_1} = \psi$$

With exposure of a thin-plate weld seam, to control the blackness of the parent material zone and the weld seam zone within the standard stipulated range, the relation of $\psi' > \psi$ should be noted when selecting the feasible tube voltage. Because from the light exposure curve in the figure, the slant lines representing the lower tube voltage have the greater inclination; therefore, with the same thickness difference for the exposure the ratio of light exposure received by the film with lower tube voltage should be greater than the ratio of light exposure received by the film for higher tube voltage, as shown in Fig. 11. However, the tube voltage should not be selected too high; otherwise, although the range of black on the negative can meet the requirements, yet the sensitivity of the image quality meter may possibly not attain the requirements. In the best case, the ratio of light exposure ψ generated after the selected tube voltage penetrating the maximum thickness difference, and the ratio of light exposure ψ corresponding to the stipulated

blackness range on the performance curve are generally the same (strictly speaking, situations in 4 in the following should be considered) [1, 2].

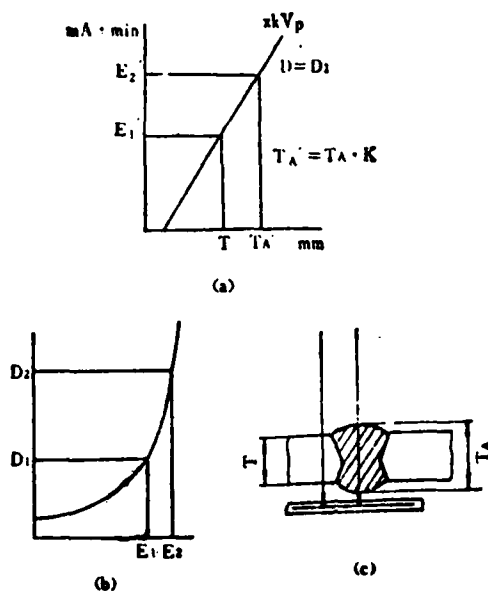
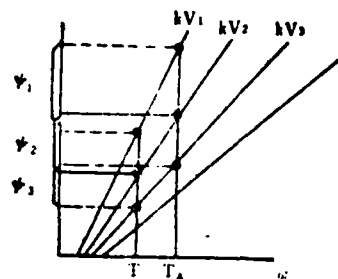


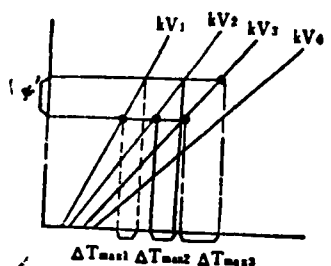
Fig. 10. Consideration of ΔT_{\max} when selecting visible tube voltage

For example, D_7 film is used for exposure of an annular weld seam with residual height 4mm and plate thickness 10mm. It is required that $K=1.1$; how much tube voltage kV_p should be selected in order to let the negative within the range of blackness between 1.5 and 3.5? The performance curve and the light exposure curve for the film used are found at the close of the article; in both cases, the related conditions are consistent.

From the performance curve of D_7 film, it is known that the corresponding logarithmic difference of light exposure for negative blackness of 3.5 and 1.5 is $2.58-2.20=0.38$. Therefore, the ratio of light exposure is $\psi = E_{3.5} / E_{1.5} = 2.4$.



(a) ΔT_{\max} 一定时, 若 $kV_1 < kV_2 < kV_3$,
则 $\psi_1' > \psi_2' > \psi_3'$



(b) ψ 一定时, 若 $kV_1 < kV_2 < kV_3$,
则 $\Delta T_{\max 1} < \Delta T_{\max 2} < \Delta T_{\max 3}$

Fig. 11. Interrelation between thickness difference and light exposure ratio

Remark: (a) for ΔT_{\max} is constant, if

$kV_1 < kV_2 < kV_3$, then $\psi_1' > \psi_2' > \psi_3'$

(b) for ψ is constant, if $kV_1 < kV_2 < kV_3$,
then $\Delta T_{\max 1} < \Delta T_{\max 2} < \Delta T_{\max 3}$

Since $K=1.1$, the maximum exposure thickness $T_A' \approx T_A \cdot K = (10+4) \times 1.1 = 15.4\text{mm}$.

Then the figure showing the light exposure curves is referred to in order to find the ratio of the corresponding light exposure ψ' of different tube voltages and thicknesses of 10mm and 15.4mm, as shown in Fig. 1.

TABLE 1

管电压 kV. 1	$T_A'=15.4\text{mm}$ 部分的曝光量 E_1 2	$T=10\text{mm}$ 部分 的曝光量 E_2 3	曝光量之比 ψ' 4
140	34	9.8	3.47
150	17.5	6	2.92
160	11.5	4.5	2.55
170	7.2	3.2	2.25

KEY: 1 - Tube voltage 2 - Light exposure
 E_1 for the portion of $T_A'=15.4\text{mm}$ 3 - Light
exposure E_2 for the portion of $T=10\text{mm}$
4 - Ratio ψ' of light exposures

It is apparent that only by selecting a weld seam with minimum thickness of 15.4mm and exposure plate thickness 10mm in the condition of 170kVp, and 7mA·min, then the ratio ψ' (2.25) of the actual light exposure is smaller than the corresponding ratio ψ (2.4) of light exposure for blackness between 1.5 and 3.5; however, all the other light exposure conditions in the table are possible to have maximum blackness in the parent material zone on the negative exceeding 3.5.

3. Maximum thickness difference and corresponding blackness range

When a certain tube voltage for exposure of weld seams of a given thickness, whether or not the corresponding blackness range of the maximum thickness difference can meet the requirement, one can first obtain the ratio (ψ') of the light exposure for a certain blackness after the X-rays penetrating the maximum and the minimum thickness from the figure showing the light exposure curve; then the corresponding blackness range of this ψ' can be obtained from the corresponding film property curve.

For example, by using D₇ film and 200kV_p for exposure of an annular weld seam with a total residual height of 4mm with 28mm as the parent material thickness, it is required that $K=1.1$. Whether or not the blackness range on the negative can meet the requirements of 1.5 to 3.5 is a question.

In this example, by referring to light exposure curve, the maximum exposure thickness $T_A' \approx (28+4) \times 1.1 = 35.2\text{mm}$. From the light exposure curve, by using 200kV_p for the exposure of 35.2mm thickness, obtaining 1.5 as the blackness, the light exposure amount is 30mA·min; however, the light exposure amount is 13.5mA·min for exposure of 28mm thickness with a blackness of 1.5 obtained. Moreover, as the ratio (of the two light exposure amounts) $\psi' = 30/13.5 = 2.22$, the ratio is smaller than the ratio 2.4 of light exposure amounts of the corresponding blackness 3.5 and 1.5 from the film property curve; therefore, the negative blackness can be controlled within the range between 1.5 and 3.5.

Now the actual upper limit of the negative blackness can be obtained from the film property curve. Since the logarithm of the light exposure amount of 1.5 blackness is 2.2, and when using the condition of 200kV_p, 30mA·min for exposure of the above-mentioned weld seam, the light exposure amount received by the portion of the parent material is 2.22 (30/13.5) times the light exposure of the portion of the weld seam; therefore, a point of $\lg E_2 = 2.2 + \lg 2.22 \approx 2.55$ can be obtained from the horizontal coordinate of the film property curve. From the point, a perpendicular line is drawn upward to intersect with the curve at a point. From this point of intersection, the corresponding blackness is 3.0.

Conversely, of course the maximum thickness difference allowed from the stimulated blackness range can be obtained by determining the exposure given the thickness.

For example, by using 180kV_p for the exposure of an annular weld seam with plate thickness of 20mm, the allowable maximum thickness ratio can be obtained from the following in order to satisfy the condition of 1.5 to 3.0 for the negative blackness:

First, from the film property curve the ratio ψ of the corresponding light exposure amount of blackness 3.0 and 1.5 can be obtained from the film property curve

$$\therefore \lg E_{3.0} - \lg E_{1.5} = 2.5 - 2.2 = 0.3, \therefore \psi = \frac{E_{3.0}}{E_{1.5}} \approx 2$$

From the light exposure curve, after using 180kV_p for the exposure of 20mm in thickness, the light exposure amount for blackness 1.5 is 9.5mA·min. To raise the blackness of the parent material to 3.0, twice the light exposure amount (9.5x2=19mA·min) should be given. From the light exposure curve it is known that the corresponding thickness is 25mm for 180kV_p and 19mA·min. Therefore, the allowable maximum thickness $\Delta T_{\max} = 25 - 20 = 5\text{mm}$. At this time, $K_{\max} = \frac{T_A'}{T} = \frac{25}{20} = 1.25$, $K = \frac{T_A'}{T_A} = \frac{25}{20+4} \approx 1.04$

For exposure according to the above-mentioned conditions, the K value can be controlled only at 1.04. If an exposure is made according to the condition K=1.1, some other tube voltage will be used.

4. Maximum thickness ratio and the allowable variation of light exposure

In actual exposure, for exposure by selecting a certain tube voltage and light exposure amount, for the maximum thickness ratio allowed to satisfy the stipulated blackness range, the following should also be considered: the deviation of focal length related to the position of the X-ray machine, and the variations of light exposure amount caused by the variation of the power supply voltage [4]. If this point is not considered,

disadvantages of overly high or overly low blackness will be the result in a large number of radiographic processes.

For example, as specified by the GB 3323-87 Standard, the blackness range is 1.2 to 3.5 for grade AB photographic method. If from the X-ray film property curve used, the corresponding ratio of the light exposure amounts of the above-mentioned blackness range is approximately 2.63 times (from $\lg E_{3.5} - \lg E_{1.2} = 2.57 - 2.15 = 0.42$; thus $E_{3.5}/E_{1.2} \approx 2.63$), and assume that the variation is plus or minus 20% in the light exposure process, then for the selected tube voltage and the light exposure amount, after the X-rays penetrate the maximum and the minimum thicknesses, to the light exposure amount received by the film should be added, respectively, the variation of plus or minus 20%, then the ratio $\psi' \leq 2.63$ of the light exposure amount; then the film can consistently meet the conditions of blackness above 1.2 and lower than 3.5.

As shown in Fig. 12, it is assumed that the light exposure amounts corresponding to 1.2 and 3.5 blackness are, respectively, E_1 and E_2 ; however, the different light exposure amounts are, respectively, E_1' and E_2' , due to the maximum exposure thickness difference when the deviation of actual light exposure amount is plus or minus 20%, then

$$E_1 = E_1' (1 - 20\%) \quad (1)$$

$$E_2 = E_2' (1 + 20\%) \quad (2)$$

When Eq. (2) is divided by Eq. (1), we obtain

$$\frac{E_2}{E_1} = \frac{E_2'}{E_1'} \cdot \frac{1.2}{0.8}$$

$$\therefore \frac{E_2}{E_1} = 2.63$$

$$\therefore \frac{E_2'}{E_1'} = 2.63 \times \frac{0.8}{1.2} \approx 1.75$$

It is apparent that the actual light exposure amount should be controlled within 1.75 times. Correspondingly, the target blackness should be 1.5 to 3.0 by consideration of the light exposure variation of plus or minus 20% as stipulated in the flaw

detection technique card.

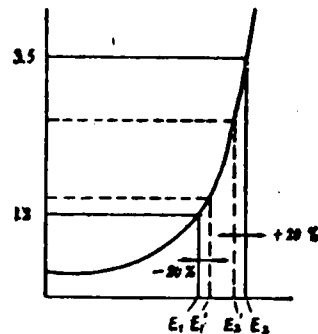


Fig. 12. Relation between maximum thickness difference versus light exposure variation amount and blackness range

From the foregoing discussion of the relation between the maximum thickness difference and the light exposure amount, of course the relation is not exact, because during actual exposure there are different situations for the scattering ratio caused by the residual height shape of the weld seam, and the situation of trapdoor shaped level plate when plotting the light exposure curve, however, this still has some significance by utilizing the approximate rule for control and revising the light exposure conditions.

VI. Conclusions

During X-ray photography of weld seams, the maximum distortion angle for controlling the K value and controlling the image and the detection rate of lateral-direction cracks at the terminal portion of a workpiece have practical significance. To satisfy the requirements of a certain K value, the effective

exposure length for each light exposure of 100% examination of annular weld seams should be properly calculated. Generally, a weld seam has a residual height; when controlling the maximum K value, there is a direct significance for tube voltage and light exposure amount required to control and satisfy the blackness range and the requirement of sensitivity of the image quality meter. By combining and utilizing the basically consistent condition of the light exposure curve and the film property curve, the maximum K value can be controlled within the range required by the level of image quality.

REFERENCES

1. Eastman Kodak Co., Radiography in Modern Industry, fourth edition, 1980.
2. Agfa-Gevaert, Industrial Radiography.
3. Deutsche Gesellschaft fur Zerstorungsfreie Prufung, Durchstrahlungsprufung fur Ingenieure (Kursus).
4. Japan Association of Nondestructive Inspection: Penetration Experiment B of Radiation Rays, 1986; Penetrating Experiment A of Radiation Rays, 1985.
5. Materialprufung, July 1984, Vol. 26, No. 7.
6. BS 2600/I-1973.
7. ISO R1106-1972.

IDENTIFICATION AND INVESTIGATION OF INCOMPLETE FUSION OF WELDS ON RADIOGRAPHS

Xin Zhongren and Ma Mingqiu, Sichuan Provincial Department of Labor and Personnel

Xin Zhongzhi, Chengdu Municipal Labor Bureau

Yang Jinjian, Neijiang Municipal Labor Bureau

Definitions and classification of incomplete fusions of welds are described. The appearance, orientation and features of incomplete fusions on radiographs are discussed and their identification methods are presented. Additionally, the main reasons for incomplete fusion are studied, based on welding methods and weld structures.

Welding is the main technique in fabricating boilers and pressure vessels; welding quality represents the fabrication quality of boilers and pressure vessels.

As is well known, the process of welding metals proceeds under conditions of thermodynamic inequilibrium. Because of the metallurgical factors of the metal materials and the specific technical factors of product manufacture, as well as the comprehensive function of structural factors due to the weldment design, especially when welding complex geometrically shaped joints and highly concentrated stressed areas, welding is a

heat treatment techniques.

In the welding process, incomplete fusion is a common technical defect with relatively serious hazards. To raise the quality of welding techniques and the useful service life of weldments, identification and overcoming of incomplete fusion becomes a problem calling for an urgent solution in welding techniques. However, it is not easy to determine correctly the images of incomplete fusion on radiographic negatives because it is very easy to be confused between the one-sided welding of root incomplete fusion and one-sided welding of root incomplete penetration. Thus, incomplete fusion is mistakenly understood as incomplete penetration, with the result that even the defect of incomplete fusion cannot be distinguished, leading to a misevaluation between incomplete fusion of edge slope and slag inclusions, and a confusion of incomplete fusion (interlayer incomplete fusion) between welding passes and slag inclusions.

On the radiographic negatives of weld seams, the image of incomplete fusion has features of a certain size, orientation, and appearance; only by mastering these features and by understanding the reasons underlying welding techniques and structures for causing incomplete fusion can one easily distinguish between incomplete fusion and other welding defects from radiographic negatives.

Definition and Classification of Incomplete Fusion

As indicated from the standard GB 3375-82, "Welding--Technical Terms," and ISO 6520, "Classification and Description of Metal Weld Seam Defects (1982)," incomplete fusion is the portion of incomplete fusion between the weld pass and the parent material or between two adjacent weld passes (or the incomplete fusion between parent material and parent material in spot welding).

According to the size of a weld seam, incomplete fusion can be divided into the following: incomplete fusion of the slope edge, incomplete fusion between weld pass and parent material (Fig. 1); interlayer incomplete fusion between two adjacent weld passes (Fig. 2); as well as incomplete fusion at the root of the weld seam, and incomplete fusion between two parent materials of the weld pass and the dull side of the slope edge (Fig. 3).

Based on the fact of whether or not slag inclusions accompany this defect, incomplete fusion also can be divided into: white incomplete fusion (incomplete fusion with no slag inclusions); black incomplete fusion (also called slag inclusion type incomplete fusion, indicating incomplete fusion of slag inclusions).

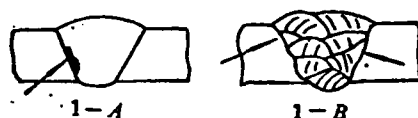


Fig. 1. Incomplete fusion of slope edge

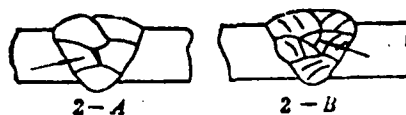


Fig. 2. Interlayer incomplete fusion

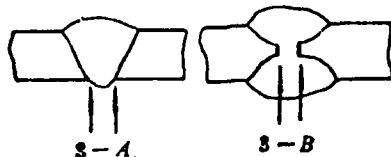


Fig. 3. Incomplete fusion at root of weld seam

Incomplete Fusion of One-sided Weld Root and Incomplete Penetration at Root

One-sided incomplete fusion at a weld root indicates the sides have no fusion or incomplete fusion between the bottom weld beam and the dull side of the parent material. At this time, the metal at the weld seam has filled the gap of the dull side, and the weld beams at the back are higher than the parent material.

As verified by experiments, whether white or black incomplete fusion, visible images can be left on the radiographic negatives; these images can be examined with radiography. This is because incomplete fusion or incomplete melting occurred at the dull side of the parent material slope edge; the dull side in the case of incomplete fusion or incomplete melting leaves a regular image on the photographic negatives.

Incomplete fusion at the root in one-sided welding leaves a visible and characteristic image on the radiographic negatives; at the dull side of the weld seam slope edge, there are regular long, slender, black lines in the longitudinal direction of the weld seam.

Because in this situation, the root of the weld seam is higher than the parent material, therefore if one examines only the appearance of the weld test plate, it can be concluded that the formation at the back of the weld seam is acceptable; the root of the weld seam is not only thoroughly penetrated, but also is free of the incomplete fusion defect. From the radiographic negatives, there is a relatively bright region at the gap of the weld seam root; this also indicates that the back surface of the weld seam has been thoroughly penetrated since the weld seam metal is higher than the parent material. However, if one closely observes the radiographic negatives, it can be discovered

that regular long, slender, black straight lines appear in the longitudinal direction of the weld seam at the dull side of the weld seam slope edge (refer to Fig. 4).

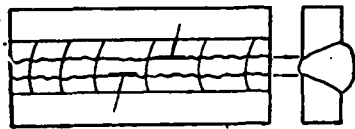


Fig. 4. Incomplete fusion at root in one-sided welding

After dissecting a weld seam test specimen and conducting a metallographic inspection on the lateral cross-section of the test specimen (refer to Fig. 10), it can be determined that the incomplete fusion defect at the weld seam root occurs when regular long slender black lines appear in the radiographic negatives.

In the case of incomplete penetration at the root in one-sided welding, since the weld seam root has not been thoroughly penetrated, all or part of the weld seam metal at the root is not higher than the parent material from a visual examination of the weld test plate appearance; at the dull edge of one or two sides of the root of the parent material there is incomplete penetration, with the persistence of the dull edge. When observed from the radiographic negative, a regular relatively complete black band (Fig. 5) appears at the gap of the weld seam root along the longitudinal direction of the weld seam; this also indicates incomplete penetration at the weld seam root.

Therefore, in the case of incomplete fusion of the weld seam at the root in one-sided welding, the weld seam root is thoroughly penetrated; however, incomplete fusion exists between

weld seam metal and the parent material metal at the weld seam root; in other words, no intracrystalline bonding occurs.

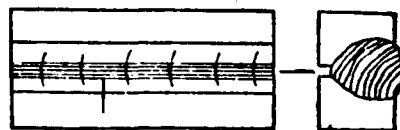


Fig. 5. Incomplete penetration of root in one-sided welding

Incomplete Fusion at Root in Double-sided Welding

Incomplete fusion at the root in double-sided welding occurs at the dull side of the weld seam slope edge, with X or I slope edge, see Fig. 3B. As verified in experiments, whether white or black incomplete fusion there is a clear image in the radiographic negative; this kind of image can be examined by the radiographic method.

Incomplete fusion at the root in double-sided welding produces well-defined images in the radiographic negative; at the dull side of the weld seam slope edge, in the longitudinal direction of the weld seam, the image is a regular long, slender, black straight line (refer to Fig. 11).

Incomplete fusion and incomplete penetration at the root in double-sided welding are two kinds of defects with different properties. Incomplete penetration at the root in double-sided welding is due to incomplete, or only partial overlapping of the weld seam metal at the weld pass of the front and reverse side, thus the parent material at the root of the weld seam is incompletely penetrated, forming the defect. In this situation, there are gaps between two weld passes at the front and reverse sides; therefore, a regular, relatively coarse black straight

line appears in the radiographic negative for the case of incomplete penetration.

However, incomplete fusion of double-sided weld root portion is due to overlapping of the metals at the front and reverse side weld passes. However, due to insufficient energy in the welding rod, although the gap of the weld seam slope edge is filled with weld seam metal, yet the dull side of the parent material has not been melted or is incompletely melted; thus, there is no intracrystalline bonding because there is only mechanical contact between the weld seam metal and the parent material at the dull side. Since there is no gap at the weld seam root, no regular long, slender, black lines are melted at the root portion in double-sided welding (refer to Fig. 11).

Interlayer Incomplete Fusion and Slag Inclusions

Interlayer incomplete fusion (Fig. 7) is also called incomplete fusion between weld passes, mostly occurring in multilayer welding. As verified in experiments, in the situation of Fig. 2A, only black incomplete fusion is visually detectable in the radiographic negative. However, white incomplete fusion cannot be examined with radiography, but only by means of another flaw detection method for inspection (such as ultrasonic flaw detection), because white incomplete fusion in this situation is similar to lamination, lapping or folding defects in steel plates.

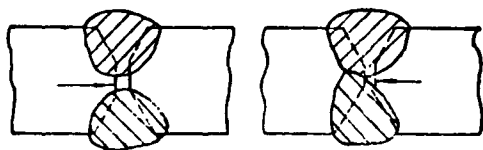


Fig. 6. Incomplete penetration of double-sided welding

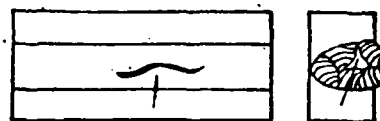


Fig. 7. Interlayer at root incomplete fusion

In the situation of Fig. 2B, as verified with experiments, whether white or black incomplete fusion, it can be inspected with radiography because gaps are present between weld passes, even in the case of white incomplete fusion, yielding visible images on the radiographic negative.

For black interlayer incomplete fusion, this is also a planar type defect; so the image on the radiographic negative has features of these two kinds of defect owing to the existence of slag inclusions and incomplete fusion; thus, there are block or stripe-shaped irregular black shadows on the radiographic negative similar to slag inclusions. However, the shade of the black image is relatively light, with uneven black and white distribution inside. The edge is relatively blurred, not well-defined and lacking a regular shape. However, the slag inclusion defect at a weld seam is a three-dimensional type defect, although there is no fixed shape displaying a black shadow on the radiographic negative; however, in the general situation the color of the image on the radiographic negative is relatively dark, basically with consistent blackness and relatively well-pronounced outlines.

Slag inclusions situated between welding passes can be treated as incomplete fusion of slag inclusions. However, slag inclusions in each welding pass cannot be treated as incomplete fusion.

Radiographic flaw detection personnel can fabricate an interlayer incomplete fusion test plate of butt weld seam according to the specific welding technique prior to radiographic exposure. In addition, comparative observations and analysis between the typical weld seam interlayer incomplete fusion radiographic negative and the slag inclusion negative should be

carried out for familiarization with the features of these two defect images and the difference in appearance and shape in order to determine correctly and distinguish these two types of weld defects through radiographic inspection.

Incomplete Fusion and Slag Inclusion at Slope Edge

For incomplete fusion of a slope edge in the situation of Fig. 1A, as verified by experiments, only black incomplete fusion can have an image persisting on the radiographic negative; however, white incomplete fusion cannot be radiographically examined, but only by adoption of another flaw detection method (such as ultrasonic flaw detection), because under this situation, white incomplete fusion is similar to lamination, lapping or folding defects in steel plates.

In the Fig. 1B situation, as verified experimentally, whether white or black incomplete fusion, it can be radiographically examined because even though it is a case of white incomplete fusion, there are gaps between the weld pass and the slope edge of the parent material enabling a visible image to remain in the radiographic negative.

Black incomplete fusion of a slope edge can have the following clear images on the radiographic negatives: on the side of the longitudinal direction central line of the weld seam, there are regular long, slender black lines in the longitudinal direction of the weld seam. Sometimes, at both sides of the central line of the weld seam there are regular, long, slender black lines in the longitudinal direction of the weld seam.

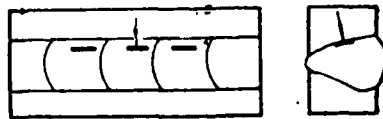


Fig. 8. Incomplete fusion at slope edge

Interlayer Incomplete Fusion and Edge Incomplete Fusion

Sometimes there is incomplete fusion at the edge when there is interlayer incomplete fusion. Interlayer incomplete fusion and edge incomplete fusion defects have typical features in the radiographic negative in that they are distributed longitudinally along the weld seam on one side of the weld seam center line.

Near the weld seam edge, it is the regular black line; however, it is the irregular black stripe facing the central line of the weld seam.

As verified experimentally, the regular black line shows up as the image of edge incomplete fusion, but the irregular black stripe shows up as the image of interlayer incomplete fusion. It should be pointed out that all incomplete fusion in this situation is black incomplete fusion, or with the existence of a gap.

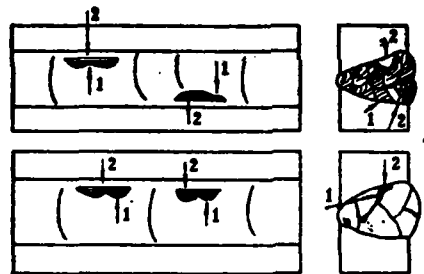


Fig. 9. Interlayer incomplete and edge incomplete fusion

Remarks: 1 - Interlayer incomplete fusion 2 - Edge incomplete fusion

Cause of Incomplete Fusion and Its Prevention and Treatment

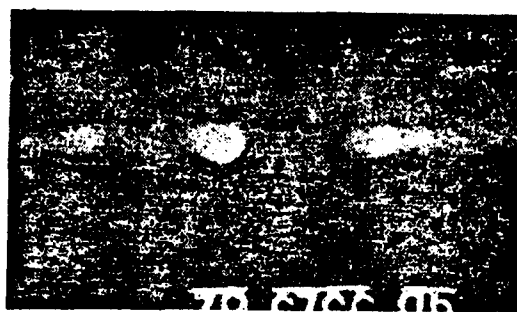
For the fusion welding method (manual electric arc welding, submerged arc welding, gas-protected welding, and electroslag welding, among other types), the main cause of incomplete fusion is the undersupply of energy to the welding rod.

For example, in the case of manual electric arc welding, in carrying out the first welding pass for a single V-slope edge butt weld seam one-sided welding, due to inappropriate welding rod motion, the electric arc deviates to one side of the slope edge of the parent material, then the slope edge at another side of the parent material is covered with filler metal prior to fusion, thus causing incomplete fusion at the root. In this situation when the welding rod energy is too small and incomplete fusion is caused at both sides of the root of the slope edge of the parent material.

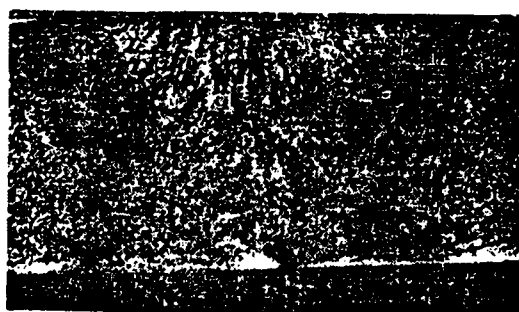
When multilayer welding is conducted with submerged-arc automatic welding, when the automatic welding speed of the submerged arc is suddenly increased, the welding rod energy will suddenly drop. Then interlayer incomplete fusion is the result, between the front layer of the weld seam and the rear layer of the weld seam.

According to GB 3323-87 Standard, Classification Method for Steel Weld Seam Radiographic Pictures and Negatives, any kind of incomplete fusion is an unacceptable welding defect; once incomplete fusion occurs in a weld seam, on the one hand the cause of the incomplete welding defect should be analyzed in order to avoid another occurrence of the defect. On the other hand, the incomplete fusion should be cleared with supplementary welding.

Typical Pictures of Incomplete Fusion Defects



(a) 射线照片



(b) 焊缝横断面



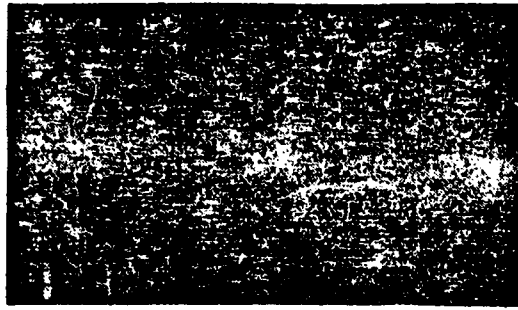
(c) 焊缝横断面

母材	1	钢板	2	焊材	3	牌号	4	焊接	5	焊缝	6	缺陷	7	透照	8
16MnR		14mm		E5015		平焊		V		手工		未熔合		150kV	

Fig. 10. Incomplete fusion at root of one-sided welding

Remark: (a) Radiographic picture (b) Cross-section of weld seam (c) Cross-section of weld seam

KEY: 1 - Parent material 2 - Thickness of steel plate 3 - Grade number of welding material
4 - Welding site 5 - Weld seam 6 - Welding method 7 - Defect type 8 - Exposure norm
9 - Level welding 10 - Manual welding 11 - Incomplete fusion



(a) 射线照片



(b) 焊缝横断面



(c) 焊缝横断面

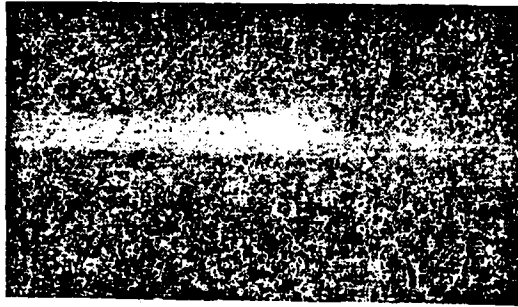
母材	1	钢板	2	焊材	3	焊丝	4	焊位	5	焊接	6	缺陷	7	透照
厚度	牌号	位置	代号	方法	种类	规范								
16MnR	16mm	E5015	平焊	×	手工焊	未熔合	150kV							

Fig. 11. Incomplete fusion at root in double-sided welding

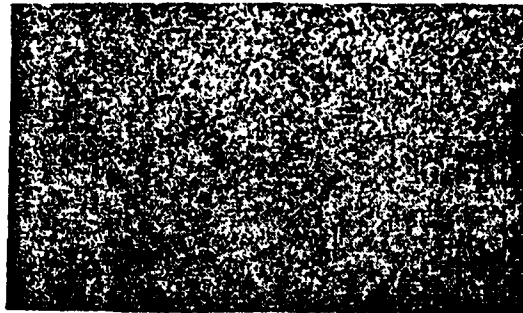
Remark: (a) Radiographic picture

(b) Cross-section of weld seam (c) Cross-section of weld seam

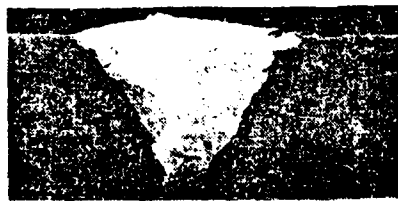
KEY: 1 - Parent material 2 - Thickness of steel plate 3 - Grade number of welding material 4 - Position of welding 5 - Weld seam number 6 - Welding method 7 - Defect type 8 - Exposure norm 9 - Level welding 10 - Manual welding 11 - Incomplete fusion



(a) 射线照片



(b) 焊缝横断面



(c) 焊缝横断面

母材 ¹	钢板 ² 厚度	焊材 ³ 牌号	焊接 ⁴ 位置	焊缝 ⁵ 代号	焊接 ⁶ 方法	缺陷 ⁷ 种类	透照 ⁸ 规范
16Mnrg	12mm	E5015	平焊 ⁹	V	手工焊 ¹⁰	未熔合 ¹¹	130kV

Fig. 12. Incomplete fusion of slope edge

Remark: (a) Radiographic picture

(b) Cross-section of weld seam (c) Cross-section of weld seam

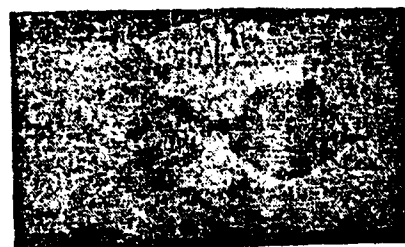
KEY: 1 - Parent material 2 - Thickness of steel plate 3 - Grade number of welding material 4 - Position of welding 5 - Weld seam number 6 - Welding method 7 - Defect type 8 - Exposure norm 9 - Level welding 10 - Manual welding 11 - Incomplete fusion



(a) 射线照片



(b) 焊缝横断面



(c) 焊缝横断面

1	2	3	4	5	6	7	8
母材	钢板 厚度	焊材 牌号	焊接 位置	焊缝 代号	焊接 方法	缺陷 种类	透照 规范
20g	11mm	E4315	平焊 ⁹	V	手工焊 ¹⁰	未熔合 ¹¹	145kV

Fig. 13. Incomplete fusion of slope edge

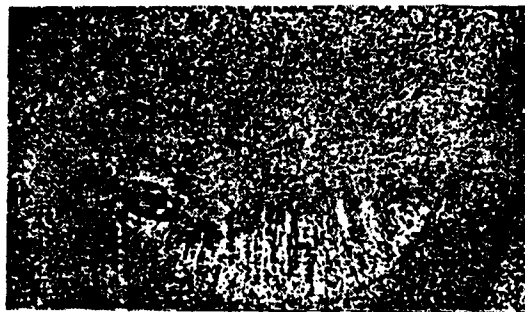
Remark: (a) Radiographic picture

(b) Cross-section of weld seam (c) Cross-section of weld seam

KEY: 1 - Parent material 2 - Thickness of steel plate 3 - Grade number of welding material 4 - Position of welding 5 - Weld seam number 6 - Welding method 7 - Defect type 8 - Exposure norm 9 - Level welding 10 - Manual welding 11 - Incomplete fusion



(a) 射线照片



(b) 焊缝横断面



(c) 焊缝横断面

母材 ¹	钢板 厚度 ²	焊材 牌号 ³	焊接 位置 ⁴	焊缝 代号 ⁵	焊接 方法 ⁶	缺陷 种类 ⁷	透照 规范 ⁸
16MnR	16mm	E5015	平焊 ⁹	V	手工焊 ¹⁰	未熔合 ¹¹	150kV

Fig. 14. Slope edge incomplete fusion and interlayer incomplete fusion

Remark: (a) Radiographic picture

(b) Cross-section of weld seam (c) Cross-section of weld seam

KEY: 1 - Parent material 2 - Thickness of steel plate 3 - Grade number of welding material 4 - Position of welding 5 - Weld seam number 6 - Welding method 7 - Defect type 8 - Exposure norm 9 - Level welding 10 - Manual welding 11 - Incomplete fusion

NEW METHOD OF NONDESTRUCTIVE TESTING OF INTERNAL STRESSES--
MAGNETIC ACOUSTIC EMISSION*

Xu Yuehuang, Du Fengmu, and Shen Gongtian, Wuhan University

Magnetic acoustic emission (MAE) refers to the generation of stress versus strain waves when a ferromagnetic material is magnetized by a varying magnetic field. MAE can be used as a new field for nondestructive testing of internal stresses. The characteristics of MAE in several kinds of finished steel products are introduced. The effects of stress, chemical composition, heat treatment and temperature on MAE are discussed. The depth that can be measured by MAE is about 3-4mm at the frequency of 50Hz. Application of the ratio of MAE values under different magnetic fields to determine internal stresses is feasible.

Foreword

The existence of internal stresses greatly reduces the bearing capacity of a structural member, thus introducing a lack of safety vector. Therefore, in production practice the internal stresses existing in a material often need to be understood. For a long time already, numerous researchers exerted their best efforts in searching for methods of detecting internal stress with precision, reliability, simplicity and feasibility.

*This is a research project funded by the Science Foundation, Chinese Academy of Sciences.

The X-ray method is reliable, since it does not damage the workpiece to be examined; the area to be examined can be selected and the method can be used to detect internal stresses in a smaller region. Shortcomings of the method are that it reveals defects in depths only tens of micrometers deep for flaw detection, complex equipment is needed, and there is inconvenience in on-site testing.

By determining precisely the propagation rate of ultrasonic waves in a material, the ultrasonic wave method can determine the magnitude of internal stresses with a short test period and instrumental portability. The method can easily serve in the inspection of surface and internal regions for internal stresses of an object; however, there are a fair number of factors affecting the results of measurements.

In addition, there are also the strain gage method, photoelastic method, Mossbauer effect and neutron diffraction, among others. There are pros and cons concerning these methods. Magnetic acoustic emission (MAE) is another new method.

Since it is affected by an alternately changing magnetic field, ferromagnetic material can emit stress, strain waves because of reciprocating oscillation of magnetic domain walls and the rotation of the magnetization vector; this is due to sonic emission. Some consider that sonic emission is related to the magnetostrictive effect; therefore, it is also called magnetomechanical acoustic emission (MAE). Measurement of internal stress with the MAE technique is based on the interdependent relation between the magnetic acoustic emission with the stress. Kusanagi et al [1] was the first to discover the close relationship between magnetic acoustic emission and stress in materials; under the condition of relatively high stress, notwithstanding the tensile or compressive stress in the material, the intensity of magnetic acoustic emission is always

appreciably lower than in the nonstress case. Ono and Shibata [2, 3] conducted a more detailed study on magnetic acoustic emission of ferronickel alloys and several types of steel; they discovered that the chemical composition, microscopic texture, stress and precooling treatment (among other factors) of the material considerably affect the magnetic acoustic emission behavior; they considered that the magnetic acoustic emission technique can possibly become a new nondestructive test method for residual stresses in structural members and other properties [4, 5].

After Ono and Shibata [3] analyzed numerous experimental results, they concluded that the main source of magnetic acoustic emission originates in the displacement variation caused by motion of 90° magnetic domain walls, and secondarily it originates from the rotation of the magnetization vector; the motion of 180° domain walls does not produce magnetic acoustic emission. The peak voltage for the MAE pulse signal is

$$V_p = C_1 \Delta \epsilon \Delta V / \tau,$$

In the equation: C_1 -- constant;

ΔV -- variation of magnetic domain volume;

$\Delta \epsilon$ -- nonelastic strain tensor in ΔV ;

τ -- rise time of signal.

Based on experimental facts, the authors made supplements to the above-mentioned model, since they considered that magnetic domain walls as such have a strain field; the process of domain wall motion will release a strain wave. Therefore, whether 90° or 180° domain wall, an elastic wave will be released upon the motion of an alternately varying magnetic field.

Abroad, at present the MAE technique has been used in the nondestructive testing of internal stresses in artillery shells, rifle barrels, and self-propelled guns, in stress testing after welding and heat treatment and in monitoring stress variations in applications of structural members. In California, some

researchers applied this method to detect internal stresses caused by thermal expansion and contraction due to cooling of steel rail [5]. Practical applications of MAE still remain to be broadly developed. The authors measured magnetic acoustic emission in several materials and discussed how MAE is affected by stress and other factors. They considered that magnetic acoustic emission can certainly become a nondestructive test method for internal stresses.

Experimental Conditions

The test specimens used were rod-shaped or strip-shaped; other than the specific heat treatment norm applied to the specimen, all others were in the annealing stage. Refer to Fig.1 for the experimental arrangement; a threaded tube was used in producing the magnetic field. For large structural members, an U-shaped yoke iron of the appropriate size can provide the magnetic field for the site to be examined. An adjustable voltage transformer provided variable current from a municipal power network at 50Hz; the acoustic emission search unit is coupled onto the test specimen. For circular test specimens, an object with a flat surface can be nailed near the specimen terminal. Vaseline was applied to couple the 100kHz (center frequency) resonance type lead zirconate piezoelectric search unit onto the site. The magnetic acoustic emission signal was converted to an electric signal by using the search unit; after amplification with a prime amplifier, filtration was applied. Upon a second amplification, the electric signal is split into a model 4429 acoustic emission instrument (made by BK Corporation for processing). The signal parameter is applied with weighted ringing. In some experiments, a Dunegan 3000 acoustic emission instrument was used; the energy rate was used as the signal parameter; the signal gain was 93dB. The AE signal and the magnetic field were fed into a recording instrument on the x - y function for continuous recording of the experimental results.

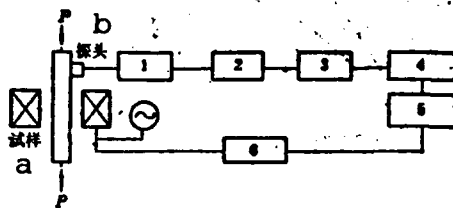


Fig. 1. Schematic diagram for MAE experimental arrangement

Remark: 1 - Primary amplification 2 - Wave infiltration 3 - Main amplification 4 - Signal processing 5 - Function recording instrument 6 - Rectification

KEY: a - Test specimen b - Search unit

Experimental Results and Analysis

1. MAE-H characteristic curve

Magnetic acoustic emission intensity increases with increase in the magnetization field, with a saturation trend. Fig. 2 shows the curve of the relationship between the energy rate of magnetic acoustic emission of a silicon-steel chip test specimen versus the applied variation of the magnetization field; the dimensions of the test specimen orientation are 300x30x0.5mm, and the grade number is Q9G. In the vicinity of a zero magnetization field, the output of the sonic emission energy rate is zero. When the magnetization field is smaller than 10A/m, the sonic emission signal can be detected; with increase in the magnetization field, first the sonic emission increases with a linear approximation. Then the emission slowly increases for a gradual saturation. In a situation with a small externally applied magnetic field, first the 180° domain walls begin to move [6]; with increase in the external magnetic field, not only do the 180° magnetic domain walls but also the 90° magnetic domain

walls begin to move by leaving the pinning points. Therefore, the energy rate of magnetic acoustic emission increases linearly. When the emission field increases further, the magnetization vector rotates. For different magnetization field intensities, each time the rotation angle $\Delta\theta$ is different; in addition, $\Delta\theta$ is affected by the magnetic crystalline anisotropy. With increase in the magnetic field intensity, $\Delta\theta$ becomes larger; therefore, the energy rate of sonic emission also increases. When the magnetic field approaches a certain value, the magnetization vector rotates to become parallel with H ; so the total energy rate of magnetic acoustic emission tends to saturation.

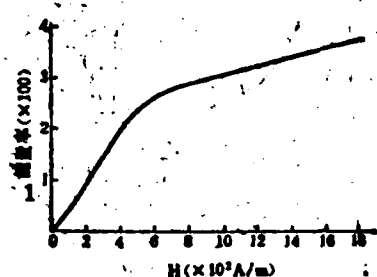


Fig. 2. Q9G MAE-H curve
KEY: 1 - Energy rate

2. Effect on MAE due to stress

Stress can appreciably reduce the magnetic acoustic emission intensity. Fig. 3 shows the relationship depicted by the MAE-H curve for steel 45. With increasing stress, the MAE-H curve is gradually lowered, but the trend of the curves is still the same. Measurements were made of the effect of magnetic acoustic emission of steel 45 and steel 20 due to stress in different grades of silicon steel and different heat treatment norms; the overall treatment is that MAE decreases with increase in tensile stress.

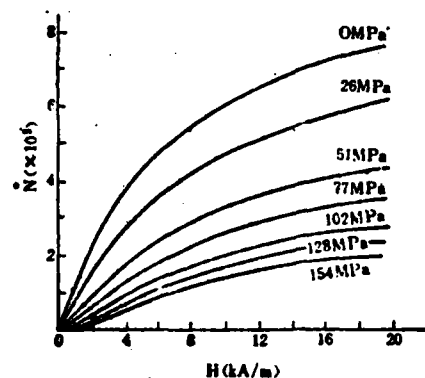


Fig. 3. Relationship curves of MAE-H for steel 40 in different stress situations

Fig. 4 shows the variation curves of MAE versus tensile stress for oriented and nonoriented silicon steel of different grades when the magnetization field is fixed at 1000A/m. Fig. 5 shows the variation of MAE versus stress for the normalizing state of steel 20 and steel 45; the acoustic emission parameter is the ringing count rate.

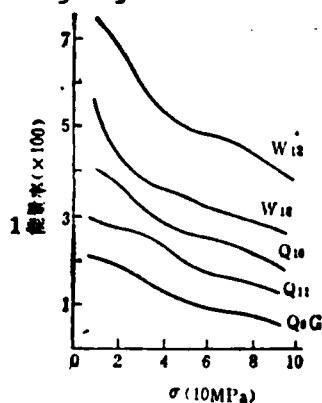


Fig. 4. MAE- σ curves for oriented and nonoriented silicon steel of steel of different grades
KEY: 1 - Energy rate

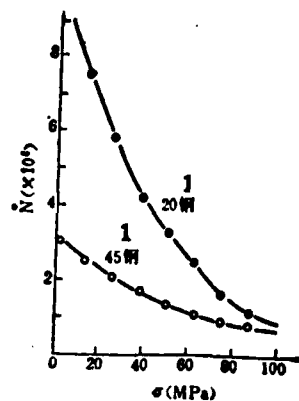


Fig. 5. MAE- σ curves for two types of normalizing steel
KEY: 1 - Steel

Fig. 6 shows the variation in the relationship of MAE versus stress for steel 45 (one case was post-annealing and the other case involved quenching at 500°C tempering). It seems that the following trend exists: for relatively simple texture of the test specimen, the closer to the equilibrium, the more MAE tends to have a steep relationship with increases and decreases in tensile stress.

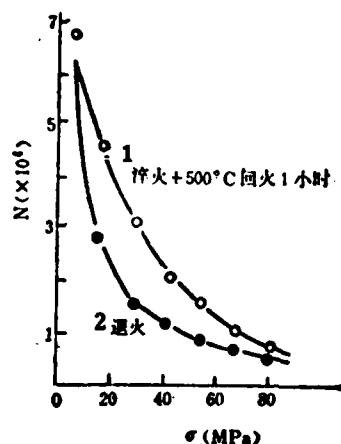


Fig. 6. MAE- σ curves for steel 45 with two heat treatment norm types
KEY: 1 - Quenching +500°C, tempering for 1 h 2 - Annealing

In addition, the curves of MAE with variation in the magnetic field (Fig. 4) for steel 45, 20CrMnTi and 20CrMnMo were plotted with the function of lower compressive stress. First, MAE increases with increasing compressive stress; after a certain peak value is reached, MAE decreases with increase in compressive pressure.

The reason for the decrease in the magnetic acoustic emission intensity with increase in tensile stress is still unclear at present. Ono et al [5] measured the variation in magnetic field intensity H_s inside a test specimen in a situation of fixed externally applied magnetic field; it was discovered

that H_S decreases in a situation of high stress. It was assumed that one of the reasons is the decrease in H_S . Luo Yang and

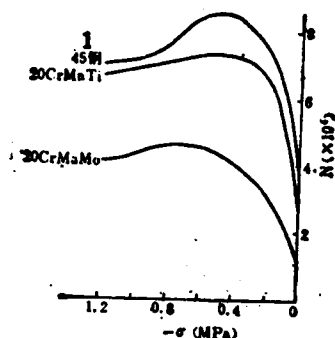


Fig. 7. Relationship curves of MAE versus compressive stress for three kinds of steel
KEY: 1 - Steel

Wang Zhenqin [7] studied the magnetic domain structure of oriented silicon steel chips and the relationship under tensile stress. It was discovered that the spacing of 180° magnetic domain walls decreases and the additional domain structure disappears on exposure to tensile stress. When the tensile stress is sufficiently high, in principle these domains become 180° strip-shaped domains. In the authors' opinion, under the action of tensile stress, the additional domain structure of oriented silicon steel disappears so that the proportion of 90° domain walls inside the material rapidly decreases. Therefore the sonic emission decreases. In addition, the 180° domain walls increase in number with a reduction in the gaps so the average free pass of the domain wall motion, thus further reducing the sonic emission.

3. Effect of other factors on MAE

Magnetic acoustic emission is highly sensitive to the following effective factors in the test material: texture,

structure, internal stress and environmental temperature.

(1) Effect of material property and texture on MAE

Magnetic acoustic emission of ferromagnetic materials is affected by numerous factors in the material: chemical composition and microscopic texture affect the magnetostrictive coefficient and the magnetic domain structure, thus causing different magnetic acoustic emission. Fig. 8 shows two MAE-H curves for annealed steel 20 and annealed steel 45 with the same shape and volume; at all magnetic field intensities, the MAE of steel 20 is stronger than for steel 45. This is because pearlites in annealed steel 45 are most numerous than in steel 20. Cementites in pearlites are nonferromagnetic; these cementites intensively impede or slow down the motion of magnetic domain walls. In Fig. 9, the components of all silicon steels are similar to each other, but differ only in crystal grain size; in addition, there is (110) <001> texture in Q₁₀ and Q₁₂. Their MAE are apparently different.

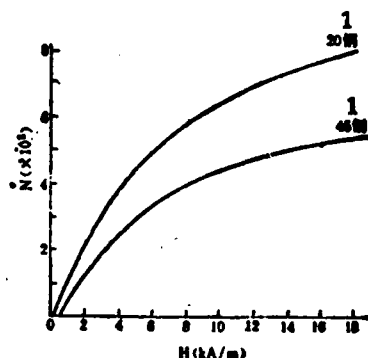


Fig. 8. MAE-H curves of annealed steel 20 and annealed steel 45
KEY: 1 - Steel

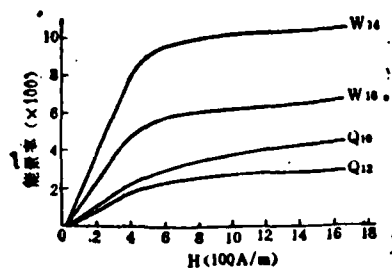


Fig. 9. MAE-H curves of oriented and nonoriented silicon steels of different grades
KEY: 1 - Energy rate

Fig. 10 shows MAE-H curves of steel 45 under different heat treatment conditions. The annealed-state magnetic acoustic emission is the most abundant. In the magnetic fields applied by the authors there was no quenched-state magnetic acoustic emission signal with higher tempering temperature, and MAE is more abundant, relatively close to the annealed-state intensity of magnetic acoustic emission.

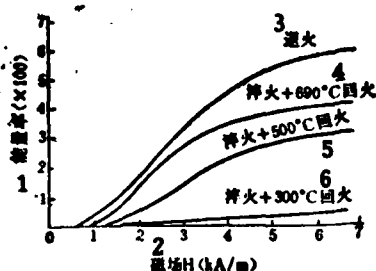


Fig. 10. MAE-H curves of steel 45 in different heat treatment conditions
KEY: 1 - Energy rate 2 - Magnetic field
3 - Annealing 4 - Quenching + 690° C tempering
5 - Quenching + 500° C tempering 6 - Quenching + 300° C tempering

When martensite texture is attained after quenching of steel, its texture stress is very high, with high-temperature

dislocations, thus affecting the domain structure and impeding domain wall displacement. Therefore, in the common range of applied magnetic fields there is no detection of magnetic acoustic emission signals. With tempering at 300° C, martensites are dissolved into highly diffused carbides; most internal stress has been eliminated, thus the displacement of magnetic domain walls becomes possible. When $H > 1200 \text{ A/m}$, the magnetic acoustic emission signal can be detected. After tempering at 500 and 690° C, carbides are gradually degraded and grow with a reduction in crystal defects and dislocation density. Thus all internal stress is eliminated and the average free path length of domain wall motion becomes larger, thus the magnetic acoustic emission increases greatly. The higher the tempering temperature the larger the cementites, the longer the free path length of domain wall motion and the more intensive is the acoustic emission. Generally speaking, the MAE is more intensive for simpler texture and structure, easier motion of domain walls, and longer free path lengths.

(2) Effect of temperature on MAE

In the process of measuring MAE, test specimens may release heat because of eddy currents. A thermocouple was affixed to a test specimen to maintain the magnetic field temperature at $1.88 \times 10^4 \text{ A/m}$, the effect on MAE (due to a temperature rise caused by eddy currents induced by the magnetic field) was measured. Fig. 11 shows a curve depicting the variation in ringing count rate of acoustic emission of steel 20 versus temperature. The value of N decreases with rise in temperature. N begins rising again after a certain temperature has been reached, then finally decreases again.

4. Stress measurement by using the ratio value method

On account of too many factors affecting MAE, there are many uncertain factors when measuring stress. Therefore a stress

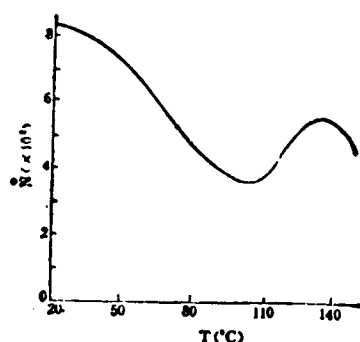


Fig. 11. MAE-T curve of steel 20

measuring method that can reduce the effects of factors has to be sought for: thus, the ratio measurement method was adopted. Refer to Fig. 3. Two fixed magnetic fields (one higher and one lower) are adopted; the ratio of MAE intensity at a higher magnetic field to MAE intensity at a lower magnetic field of each curve is used as the Y axis; the stress σ is used as the X axis for plotting curves. Fig. 12 shows the curves of ratios of MAE intensity versus stress variation at high magnetic fields ($H=16 \times 10^3 \text{ A/m}$) and low magnetic fields ($H=4 \times 10^3 \text{ A/m}$) for steel 45, steel 20, oriented silicon steel Q9G, and nonoriented silicon steel W₁₄. With increasing stress, basically the ratio values increase linearly. This indicates that there is a weaker relationship between the ratio of MAE intensity at high magnetic fields and at low magnetic field, and the relationship of macroscopic texture, by relying simply on stress. Therefore, in most cases, only with a known basic microscopic structure can this parameter be used to measure internal stress. This method can also eliminate the effects of dissimilar coupling conditions at various times.

5. Discussion on measured depths

Because of the skin effect, depth limitation exists in the test specimen, with the MAE produced in an alternately changing magnetic field. To estimate the depth, test specimens of steel 45 with the same length, strip-shaped (18x240x2mm) and rod-shaped (outside diameter 20mm) were subjected simultaneously to the annealing treatment. Under the same conditions, the count rates at saturated ringing for MAE measurements are, respectively, $7.2 \times 10^4 \text{s}^{-1}$ and $3.3 \times 10^5 \text{s}^{-1}$. The authors assumed that the entire cross section of the test specimen was magnetized; however, only the outer layer at a certain depth of the round-cross section of

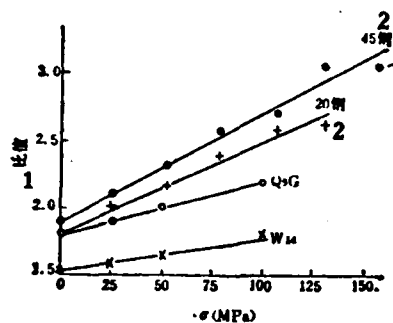


Fig. 12. Curves of MAE ratio of values versus σ

KEY: 1 - Ratio of values 2 - Steel

the rod test specimen was magnetized. Thus, it is estimated that the depth of magnetic acoustic emission is approximately 3-4mm. Ono et al [5] measured the depth at 60Hz alternately varying magnetic field and found it to be approximately 2~3mm.

Conclusions

1. Magnetic acoustic emission decreases with increase in stress.

2. The composition, texture, environmental temperature and coupling conditions of a material are highly sensitive to magnetic acoustic emission.

3. By measuring internal stress with the ratio value method, the effects of the material properties and the coupling conditions of texture can be considerably reduced; this is a feasible method for measuring internal stress by MAE.

4. The material depth at which magnetic acoustic emission is produced at a 50Hz alternately varying magnetic field is approximately 3~4mm.

REFERENCES

1. Kusanagi, H., H. Kimura and H. Sasaki, J. Appl. Phys. 50/4, 2985 (1979).
2. Ono, K. and M. Shibata, Mater. Eval. 38, 55 (1980).
3. Ono, K. and M. Shibata, Advances in Acoustic Emission, edited by H. L. Dunegan and W. F. Havtman, Dunhart, Knoxville, p. 154, 1981.
4. Ono, K. and M. Shibata, Proc. Conf. NDT, Railway Adm., American Association of Railroads, February (1979), Washington, D. C.
5. Shibata, M. and K. Ono, NDT International, 5, 227 (1981).
6. Guo Yicheng, Tieci xue [Ferromagnetism], Higher Education Publishing House, p. 440, 1965.
7. Luo Yang and Wang Zhengqin, Jinshu Xuebao [Metals], 19/2, A125 (1983).

ANALYSIS OF ABNORMAL DEFECTS ON X-RAY FILMS

Li Lanrui and Li Tongchao

The acetylene gas bottles made in the authors' plant are in the class three pressure vessel category, requiring 100% radiographic inspection. The production of the gas bottles is on a large scale so the assessment of the radiographic negatives is a labor-intensive mission, requiring nearly 5000 negatives to be assessed per day. Recently, in the assessment of negatives the authors discovered some abnormal defects, such as black-and-white rings; on the negatives there are circular rings of white at the center and black at the circumference; however, the blackness in the circle is equivalent to the normal weld seam blackness. There were disputes on the flaw detection data that could not be determined qualitatively. Some inspectors thought that these defects were gas bubbles, while other inspectors thought that these defects were due to sand inclusions, since gas bubbles are imaged with greater blackness value at the center than the periphery; for sand inclusions, the value of blackness in the circle should be slightly greater than the blackness value for a normal weld seam. Therefore, the two above-mentioned qualitative determinations are not precise enough.

Finally, through an analysis this kind of defects should be determined as the column (a part of filler wire) inclusions. This explanation has been verified after dissecting workpieces. The reason for the existence of the above-mentioned defects is

because automatic submerged arc welding was employed at the welding shop. When the welding stopped, there should have been filler wire withdrawal. Because of slight malfunctioning of the welding machine, after the operator cut off the current, the filler wire still moved forward continuously because of inertia, thus inserting the filler wire into the molten pool of the welding area. At that time, the high temperature of the molten pool of the welding area can still melt the bottom of the filler wire, but not the lateral and upper sides of the filler wire; the upper portion of the filler wire became softened because of scorching. When the operator withdrew the welding machine, the filler wire was broken; the filler wire section dropped into the molten pool, causing the above-mentioned phenomenon.



Fig. 1



Fig. 2

The solution of this problem was fed back to the welding shop by the authors to ask the welders to improve the welding technique, thus improving the welding quality.

MEASUREMENT AND LOCATION OF WELDS FOR RADIOGRAPHIC INSPECTION

Sun Wenhai, Weifang Chemical Machinery Plant

The article mainly presents relatively precise locating and methods of measuring weld seams and radiation source during an exposure.

Based on different workpiece specifications under exposure, the radiation source should be placed at the appropriate exposure position. In actual operation when there are exposures at different angles, the position of the radiation source and the cemented-on film should be precisely measured and located. The measurement procedure (Fig. 1) for weld seam exposure angles serves mainly in exposing workpieces of large diameter, as well as different height and angles. In the figure, solid lines indicate the internal exposure method; dotted lines indicate external exposure. During exposure, based on the diameter of the workpiece to be exposed, the flexible joints between a straight rod and a connecting rod are pulled in order to adhere the four-joint plate (Fig. 1) tightly in the exposure position. The central straight rod points toward the center of the radiation source and is parallel to the central indicating rod on the radiation beam window. Fig. 2 is mainly used on the occasion when the internal and external central positions at the test film of the workpiece seam under exposure cannot be easily measured (not including T- or cross-shaped weld seams). For example, in the case of the external method of weld seam exposure, the inside diameter of the workpiece under exposure can have a film cemented on it ahead of time, based on the site requiring exposure, and

the central position of the film cementing site can be drawn. Based on the calculated circumference of the outside diameter and the positioning scale coordinates, the position of the outside diameter center of the workpiece under exposure can be relatively precisely measured.

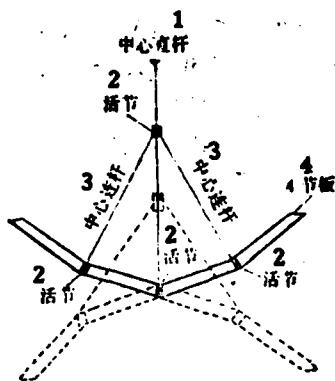


Fig. 1

KEY: 1 - Central straight rod
2 - Flexible joint 3 - Central connecting rod 4 - Four-joint plate

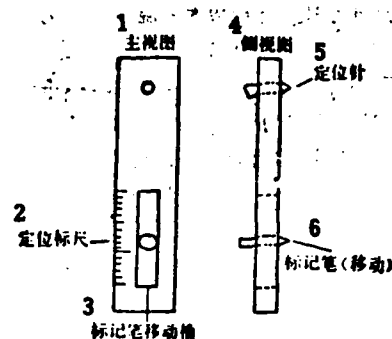


Fig. 2

KEY: 1 - Front view 2 - Locating scale 3 - Moving slot of marking pen 4 - Side view 5 - Positioning needle 6 - Marking pen (movable)

DISCUSSION ON FILM ASSESSMENT OF WELD ROOTS IN PAD WELDING

Ren Shiping, Pressure Vessel Plant, Qiancheng Industrial Corporation, Quzhou, Zhejiang

Because of improper gaps in the alignment of both sides of annular weld seams in a small-capacity vessel, molten metal flows into the pad slot (Fig. 1) during welding; thus, film assessment personnel frequently confuse incompletely welded roots, edge defect, and molten slag in the pad gap. However, there are no stipulations as to the weld seam defect of pad structure in GB 3323-82 Standard. If all these above-mentioned defects are assessed as not qualified, the repair of workpieces not only increases welding costs and work time, but also will damage the mechanical and chemical properties of the weld joints, thus affecting vessel quality and causing unnecessary losses.

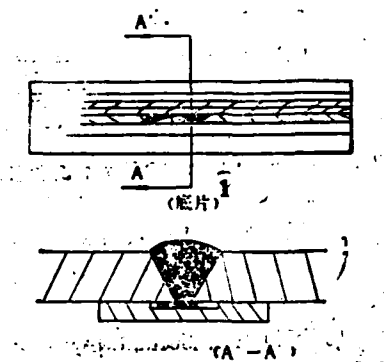


Fig. 1
KEY: 1 - Negative

As is well known, it is relatively difficult for film assessment personnel to evaluate precisely the related and unrelated defects. In the case of incomplete welding of the vessel root with pad, edge defect, and molten slag in gaps of the pad, frequently reliance is placed on the X-ray machine for macroscopic evaluation and analysis. From a large number of radiographic negatives, especially on occasions when the center of the X-rays deviates from the weld seam, it is more difficult to evaluate the related and unrelated defects. Therefore, during film assessment the main sites should be stressed; in other words, when the gap between edge openings of the parent material is too large, owing to crystalline coalescence of the filler metal of the filler wire and the pad, there are visible melting lines at the weld seam root. These melting lines are the important basis for the film assessment personnel in determining defects of incompletely welding, edge defect, and molten slag in gaps of pad. All defects falling within the melting lines can be assessed as incomplete welding at the root (Fig. 2). However, in the case of one or two black shadows at the edge of the melting line, if the shadows are of wavy shape and consistent with the trend of the weld seam waveform, this case can be treated as an edge defect of the root according to JB 741-80 Standard (Fig. 3). However, in the case of stripe-shaped slag inclusions at both sides of the melting line at the root (except the possibility of slag inclusion in the weld seam), and for the case of black shadows near the outer edge of the melting line, this case can be assessed as molten slag in gaps of pad. As the central beam of the X-ray does not deviate from the weld seam, this kind of unrelated defects does not have a great influence on welding quality. The defect grade can be leniently assessed; however, this kind of defect should be recorded in writing. If the film assessment personnel are really unable to make an assessment, the dual-shadow exposure imaging technique can be applied for a satisfactory explanation and verification of the above-mentioned problems. For a weld seam with pad, some welders are often

unable to weld satisfactorily; the main reason is in the root. Based on practice, in the opinion of the author and his colleagues, the first weld seam at the root can be welded by properly increasing the welding current to ensure a successful weld seam in a single pass without unnecessary repair, when ensuring that other factors remain unchanged.



Fig. 2
KEY: 1 - Incomplete welding

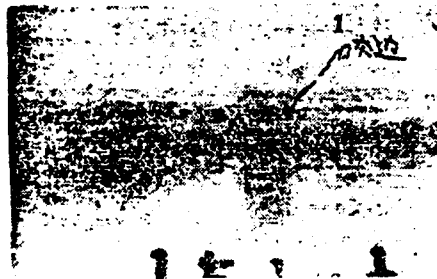


Fig. 3
KEY: 1 - Edge defect

**RULES FOR QUALIFICATION AND CERTIFICATION OF NONDESTRUCTIVE TEST
PERSONNEL--CHINESE PEOPLE'S REPUBLIC STATE STANDARD GB 9445-88**

1. Contents and Adaptation Range of Main Topic

This standard regulates the general principles and methods of personnel grade classification, duty, certification of technical qualification and issuing of certificates for the five nondestructive test (NDT) methods of ultrasonics, radiography, magnetic particles, permeability and eddy current.

This standard is adaptable to the NDT methods stipulated in this standard for certification of the technical qualifications of NDT personnel involved with industrial products, parts, components, structural members, raw materials, and supplies, as well as monitoring and examining of in-service equipment quality and safety. This standard is also adaptable to technical qualification certification by personnel administering qualification examinations for on-duty NDT personnel.

No qualification certification is required according to the technical standard on management personnel administering quality and safety control in scientific research, teaching, instruments, equipment and device production and state agencies on NDT techniques.

Those personnel who have passed the qualification certification examination are issued the Technical Qualification Certificate for NDT Personnel by the administrative department upon receiving a test report from the Qualifying Body. Only NDT personnel who have received technical qualification certificates can engage in NDT work at the corresponding grade and method as specified in the certificate they hold.

2. Technical Terms

Technical qualification is defined as the comprehension of knowledge and technique required for correctly executing the NDT mission, as well as experience and practice of NDT professional training.

Certification of technical qualification indicates the technical knowledge and capability of NDT personnel for inspecting general or special examination objects by using a certain NDT method, as well as the examination and certification process of the technical qualification. After passing the qualification test, these personnel are issued technical qualification certificates.

The Qualifying Body is a nonprofit, fair-minded agency under administrative departments; the body is responsible for execution of technical qualification certification rules for NDT personnel. The Qualifying Body authorizes a certain examination center for handling such examinations.

By filing applications, applicants of NDT candidate request by written application that they be given a qualification certification examination according to the stipulations of this standard.

Basic education is regular education recognized by the administrative departments. Basic education is one of the requirements for approved participation in qualifying examinations for NDT personnel.

NDT training is the educational process of methodological theory and practical capability of these applicants for NDT personnel. By referring to the recommended teaching outline and curriculum units, the applicants for NDT personnel qualifying examination receive training. The test specimens and reference blocks for exercises during training are not to be confused with those in the NDT examination.

Practical experience is the cumulative time of the qualifying examination applicants on certain NDT methods as their main work. Such cumulative time should be evaluated and approved. The personnel division of the examination applicants' unit is responsible for evaluating the cumulative time of the recorded practical experience.

NDT methods are certain methods of NDT applications in the relevant physical principles; these methods in the standard include ultrasonics, radiography, magnetic particle, permeability and eddy current, among other methods.

NDT techniques are the concrete execution of certain NDT stipulations on how to execute NDT methods in some NDT work procedure. Generally, such techniques are described in the NDT technical manual.

NDT procedures are documents that detail the where, when and how of the examined product for NDT work.

At present, an industrial sector is the administrative department of various production units of industrial products

under the State Council, as well as those units equivalent to the level of ministry or commission of railroads, communications and safety supervision.

General examination includes the basic knowledge that the NDT personnel should master, the fundamental principle of a certain NDT method, the basic inspection technique of general NDT objects, as well as knowledge and practical experience of the quality grade assessment standard. For NDT personnel of grade III, the general examination includes basic knowledge on materials, techniques and cause of defects, general awareness of the articles of this standard and other NDT methods, as well as practical experience of compiling general manuals of NDT processes and techniques. The level of this examination should be consistent among the various industrial departments.

An industry-specific examination is a supplementary examination on the basis of a general examination as required by an industrial department for specific reasons. Such an examination includes the operation and calibration of specific equipment used by the industrial department; specific procedures of inspection techniques, specialized norms, standards and codes as well as acceptance standards; and a compilation of specialized NDT processes and a technical manual.

A general certificate of technical qualification is issued to the NDT examination applicants who have passed the general examination with qualification approval. Such a general certificate should be recognized among various industrial departments. Only those holding the general certificate of technical qualification can go to the next step of taking part in the industry-specific examination. However, for general industrial NDT application departments, persons holding the general certificate of technical qualification can engage in NDT work of the corresponding grade and the corresponding NDT

methods.

An industry-specific certificate of technical qualification is issued to those NDT examination applicants who have passed the technical qualification industry-specific examination and with qualification approval.

The form of the basic knowledge examination is a written test with the following contents: general NDT knowledge and theory (different depths for different grades), materials, technical processes and causes of defects (for industrial department with specific requirements, this means the knowledge about materials, technical processes and causes of defects of the particular industrial department), as well as the knowledge relating to the rules of this standard. The examination contents should be included in the general examination and the industry-specific examination.

The methods examination is in the form of a written test with the following contents; principle of a NDT method, application and limitations of this method, equipment, instrument, reference block, test specimen, use of test agents, general methods, standards, norms and quality levels, as well as ability in analyzing test results. For industrial departments with specific requirements, the methods examination is the supplementary contents of the special requirements relating to the above mentioned contents.

The examination on practical ability is a test on practical operations for grades I and II by examining the applicants on their general or specific operational technique and skillfulness for a NDT method. For grade III personnel, the examination covers their capability of compiling a general or specific NDT technique and process manual in the form of a written test. In addition, through the supplementary oral examination, their

practicing capability is examined. This kind of examination contents should be included in both the general examination and the industry-specific examination.

3. Classification of Technical Qualification Grades and Technical Duty for NDT Personnel

3.1. Classification of technical qualification grades

There are the three following grades for technical qualification of NDT personnel: grade III as the highest, grade II as the intermediate, and grade I as the lowest. Qualification certification is conducted on different grades and methods.

3.2. Technical duties of various grades of NDT personnel

3.2.1. Grade I NDT personnel should have the capability under supervision and monitoring of grade II or III personnel to conduct NDT work based on a technical manual, to calibrate and use instruments, to conduct inspection operation, to record the inspection results, and to make assessment of elementary grades based on inspection results as stipulated in this standard.

3.2.2. Based on matured techniques, grade II NDT personnel can compile a technical manual, install and calibrate instruments and equipment, concretely carry out NDT work, illustrate and evaluate inspection results based on code and standard, write and sign reports on inspection results, master the adaptation range and limitations of NDT methods, as well as train and supervise grade I personnel and those not yet receiving any certificate.

3.2.3. Grade III NDT personnel should have all responsibilities on determining NDT techniques and processes, on executing stipulations in codes, norms and standards, in supervising and monitoring the overall progress of NDT work, in

illustrating and evaluating the inspection results based on codes, norms and standards, in having the capability of designing specific NDT methods, techniques and processes, in assisting the related technical departments to prescribe acceptance standard when no acceptance standard can be applied, in mastering the practical knowledge of materials, structure and production technique, in mastering other NDT methods, as well as in training grades I and II personnel.

4. Qualifying Body

4.1. Composition

The qualifying body should include representatives of the administrative department, representatives of safety and quality monitoring departments, and personnel appointed by the administrative department and those issued grade III NDT technical qualification certificates. Grade III NDT personnel should be in the majority on the examining body.

4.2. Duties

4.2.1. The examining body compiles a Collection of General Examination Questions, a Collection of Industry-Specific Examination Questions, and Examination Rules on Practical Operation Techniques, and makes reference blocks and specimens for special examinations of the general or the administrative industrial department.

4.2.2. The examining body jointly establishes an examination center with the administrative or other industrial department.

4.2.3. The body conducts a qualifying examination for grade III NDT personnel.

4.2.4. Under the requirements of the rules in this standard, the qualifying body organizes examination work for qualifying NDT personnel below grade II of this administrative department. The body authorizes and appoints examination organizations or units for qualifying NDT personnel below grade II in this administrative department.

4.2.5. The body approves the examination results of qualifying grades II and I personnel of this administrative department.

4.3. Examination center

An examination center can be authorized by the examining body for its establishment and approval; the requirements of examination center are as follows;

a. The center should have a sufficient number of working personnel (who have been approved) as well as appropriate housing and equipment facilities in order to ensure requirements of the general examination and the industry-specific examination of NDT personnel.

b. In various examination centers, the common examination reference blocks and specimens should include comparative defect types and kinds.

c. Based on requirements set by the examining body, the examination center makes reference blocks and specimens for examination; these blocks and specimens should be separated from that used in training and exercise.

5. Qualifications of Examination Applicants

5.1. General requirements

Examination applicants should have a certain level of educational and training background as well as practical experience in order to ensure sufficient understanding and skillful application of the principles, techniques and processes of NDT methods for such qualifying examinations that these applicants take part in.

5.2. Training

5.2.1. Training of grades I and II NDT personnel

Training should proceed according to the Training Outline announced by the Qualifying Body. Refer to Table 1 for the number of training hours. During application for qualifying examination, applicants should provide graduation certificates required by this kind of examination to be approved by the examination administering organization.

Table 1. Training time in hours

1 无损检测方法	2 I 级	3 II 级
4 射线照相法检验 RT	60	120
5 超声检验 UT	60	120
6 磁粉检验 MT	36	60
7 渗透检验 PT	24	60
8 涡流检验 ET	60	120

Remark: Training hours include class hours in two aspects of theory and practice. Based on different academic levels of trainee, appropriate adjustment of training hours can be made. It is appropriate to have a 50/50 distribution of training hours between theory and practice

Key: 1 - NDT method 2 - Grade I 3 - Grade II 4 - Radiographic testing RT 5 - Ultrasonic testing UT 6 - Magnetic particle testing MT 7 - Permeability testing PT 8 - Eddy current testing ET

5.2.2. Training of grade III NDT personnel

On account of technical requirements in qualification certification of grade III NDT personnel, inspection of the training resume of qualification examination applicants can apply different methods, such as the situation of taking part in a training class, situations of taking part in academic exchanges or special topic study of academic societies or industrial systems, self-study of professional books, journals as well as technical manuscripts and data. Therefore there are no specific stipulations for training hours for grade III NDT examination candidates in Table 1.

5.3. Practical experience

For cumulative hours in practical experience in inspection methods approved for qualifying examination applicants, at least the stipulated hours in Tables 2 and 3 should be attained.

Table 2. Practical experiences in years for grades I and II NDT qualifying examination applicants

1 鉴定的检测方法	UT, RT, ET		MT, PT	
2 技术等级	I	II	I	II
3 理工科大学及大专毕业生	0.50	1.00	0.25	0.50
4 高中、中专毕业生	1.00	2.00	0.50	1.00
5 初中毕业或有熟练操作证明者	2.00	3.00	1.00	1.50

KEY: 1 - Certified inspection methods
2 - Technical grades 3 - Graduates of science and engineering colleges as well as professional schools 4 - Graduates of senior high schools and secondary professional schools 5 - Graduates of junior high schools or those holding certificates of experienced operators

Applicants for grade II NDT qualifying examination should

hold a technical qualification certificate of grade I NDT personnel. For those without a qualifying certificate of grade I NDT personnel and applying for the qualifying examination of grade II NDT personnel, practical experience time should be the summation of resume time for grades I and II personnel.

Table 3. Practical experience in years for grade III qualifying examination applicants

a. 理工科本科大学毕业生*	1 具有Ⅱ级证书者	2 没有Ⅱ级证书者
	1	2.5
b. 理工科大学专科毕业生*	2	3.5
c. 其他文化程度具有Ⅱ级证书者	4	

Remark: For those qualifying examination applicants who are graduates of NDT specialty of science and engineering colleges, the practical experience time can be shortened by one-half

KEY: a - Graduates of science or engineering college b - Graduates of special professional class of science and engineering colleges c - Those of other academic level but holding qualifying certificate of grade II NDT personnel

1 - Those holding certificate of grade II NDT personnel 2 - Those without certificate of grade II NDT personnel

5.4. Requirements on vision

Those qualifying examination applicants should hold a vision certificate issued by a hospital with the following vision requirements:

- a. Corrected or uncorrected vision should equal at least

20/30.

b. It is required that the corrected or uncorrected myopia should be able to read number Jaeger 2 letters or equivalent pattern and size; the distance between the tested eye and the standard Jaeger examination chart should not be less than 30 cm.

c. The color distinguishing ability of the qualifying examination applicants should be able to distinguish color contrast related to NDT methods.

6. Examination

6.1. Examination contents

Stipulated in this standard, the examination contents of every NDT method should include three aspects of basic knowledge, methods knowledge and practical ability.

The examination contents include two examination series: General Examination and Industry-Specific Examination. The level of General Examination should be consistent among various industrial departments.

6.2. Qualifying examinations for grades I and II NDT personnel

6.2.1. Contents of General Examination

General Examination for qualifying grades I and II NDT personnel include basic NDT knowledge and its application techniques, practical inspection ability on general NDT objects, as well as degrees of understanding and mastering the quality level classification and assessment standard in addition to common NDT methods and safety protection.

The written test part in the General Examination (in other words, the test depth and extent of Basic Knowledge and Methods Knowledge) should not exceed the level of the Collection of General Examination Questions as promulgated by the Qualifying Body for reference by applicants of these examinations.

The number of questions in the qualifying examination should at least equal the number listed in Table 4.

Table 4. Number of questions in General Examination

1 无损检测方法	2 I 级	3 II 级
5 超声检验 UT	40	40
4 射线照相检验 RT	40	40
6 磁粉检验 MT	30	30
7 渗透检验 PT	30	30
8 涡流检验 ET	30	30

KEY: 1 - NDT method 2 - Grade I
 3 - Grade II 4 - Ultrasonic test
 UT 5 - Radiographic test
 RT 6 - Magnetic particles test
 MT 7 - Permeability test PT
 8 - Eddy current test ET

The practical ability part in the General Examination includes examining test applicants' operation capability with instruments and equipment, ability to analyze the inspection information obtained and to explain correctly the inspection results, the ability of qualifying examination applicants to ensure inspection results, reliability and effectiveness (such as mastering, applying and calibrating reference blocks and image quality meters as well as sensitivity test sheets and contrast reference blocks in permeability inspection), as well as the inspection and quality level assessment ability on general inspection objects, such as conventional castings, forgings, rolling workpieces and welding workpieces, among others.

6.2.2. Contents in Industry-Specific Examination

The Industry-Specific Examination for qualifying grades I and II NDT personnel includes NDT knowledge and techniques by imposing special requirements on industrial products and objects by evaluating examination applicants in a supplementary test with respect to practical inspection ability, as well as their mastering of the special standards, norms and grade evaluation methods.

In the written test part test (that is, test for Basic knowledge and Methodology Knowledge) in the Industry-Specific Examination, its depth and extent should exceed the level in the Collection of Industrial Specific Examination Questions as promulgated by the Qualifying Body for examination reference. The number of examination questions should equal at least the number listed in Table 5.

Table 5. Number of questions in Industry-Specific Examination

1 无损检测方法	2 I 级	3 II 级
4 超声检验 UT	20	20
5 射线照相检验 RT	20	20
6 磁粉检验 MT	20	15
7 渗透检验 PT	20	15
8 涡流检验 ET	15	15

KEY: 1 - NDT method 2 - Grade I
3 - Grade II 4 - Ultrasonic test
UT 5 - Radiographic test RT 6 -
Magnetic particle test MT 7 -
Permeability test PT 8 - Eddy
current test ET

The practical ability part in the Industry-Specific Examination includes approval of applicants' operational ability with specialized instruments required in testing, testing ability based on specialized standards, techniques and processes; ability

on mastering the specialized acceptance standards, assessing test results and classifying quality levels.

6.2.3. General assessment

General assessment of the General Examination and the Industry-Specific Examination should be conducted separately. For those qualifying examination applicants who passed the General Examination with a certificate issued, such qualification should be recognized by other industrial departments; the repeated examination on general knowledge and technique is exempted.

The examination mark of each item of qualifying applicants should be graded in percentage system. The passing mark on written and operation tests should be at least 70 percent.

General assessment of various test marks is determined by the summation of weighted coefficients. Refer to Table 6 for the weighted coefficients.

Table 6. Weighted coefficients in general assessment of grades I and II NDT qualifying personnel

1 等级	2 通用考试		3 工业部门考试	
	4 笔试	5 实践考试	4 笔试	5 实践考试
I	0.4	0.6	0.4	0.6
II	0.5	0.5	0.5	0.5

KEY: 1 - Grade 2 - General Examination 3 - Industrial Specific Examination 4 - Written test 5 - Practical test

Summation of weighted coefficients in General Examination and Industrial Specific Examination should equal to 1.0 in each case. At the General Assessment, a passing mark should be at

least 80 percent.

6.3. Qualifying examination for grade III NDT personnel

6.3.1. The qualifying examination for grade III NDT applicants is in written form. In addition, verification of applicants' technical qualification and an oral test on technical capability should be conducted.

6.3.2. Contents in General Examination

6.3.2.1. Basic Knowledge (Only one test is required when verifying several methods)

a. Five examination questions related to the contents of this rule.

b. Fifteen examination questions related to knowledge of common materials, strength of materials, product manufacturing process, defect property and defect causative mechanism.

c. Twenty examination questions corresponding to the level of the Collection of General Examination Questions for qualifying grade II NDT personnel of four other NDT methods thus promulgated.

6.3.2.2. Methods knowledge

a. Thirty examination questions with a level corresponding to the Collection of General Examination Questions thus promulgated for grade III personnel on NDT methods; and

b. Ten examination questions on ability in explaining the related codes, standards and technical norms for NDT methods.

6.3.2.3. Practical ability

It is required that the qualified (from the examination) NDT personnel have the ability of compiling NDT process and technical manual for conventional test objects. For applicants of the qualifying examination not yet having a grade II qualification certificate, they should be tested additionally on practical operational techniques of this NDT method.

6.3.3. Contents in Industry-Specific Examination

6.3.3.1. Twenty examination questions corresponding to the level of the Collection of Examination Questions on Methods Knowledge in the NDT test of Basic Knowledge for grade III personnel required by the specific industrial department and promulgated by the Qualifying Body. The range of such examination questions include the manufacturing technique of special materials and products used by the specific industrial department, defect property, defect causative mechanism, as well as the specific norms, standards and codes of NDT method that the qualifying examination applicants requested in addition to the specific inspecting instruments, methods, techniques and processes.

6.3.3.2. In the Industry-Specific Examination, it is required in the Practical Ability test of grade III NDT qualifying personnel with the ability of compiling an NDT process and a technical manual on specific test objects of the industrial department. For such qualifying examination applicants not yet obtaining a grade II technical qualification certificate of the administrative industrial department, an additional test is required on the practical operational technique of the NDT method.

6.3.4. General Assessment

General assessment of the General Examination and the Industry-Specific Examination should be conducted separately. Upon passing the General Examination and being issued a qualifying certificate, it should be recognized by other industrial departments without a repeated test on general knowledge and technique.

Each test item of the qualifying examination of applicants should be graded in mark of percentage system. An applicant's mark on the written test should be at least 70 percent. On not passing the operations and techniques test for grade II NDT qualifying certificate, the applicant's test mark is considered as not passing the test of practical experience (in other words, considered as a mark below 70 percent).

General assessment of all test marks is determined as the weighted coefficient summation of all items.

Refer to Table 7 for the weighted coefficients during assessment of grade III NDT qualifying examination.

Table 7. Weighted coefficients for grade III NDT personnel during general assessment

1 通用考试			2 工业部门考试	
3 基础知识	4 方法知识	5 实践能力	3 基础知识及 4 方法知识	5 实践能力
0.35	0.35	0.30	0.60	0.40

KEY: 1 - General Examination 2 - Industrial Specific Examination
 3 - Basic knowledge 4 - Methods knowledge 5 - Practical experience 6 - Basic and Methods knowledge

Summation of weighted coefficients should be 1.0. During

general assessment, the passing mark of qualifying examination applicants should be at least 80 percent. If doubts are raised on technical qualification and experience during an oral test of the qualifying applicants, a written opinion is filed after an evaluation meeting by the Qualifying Body.

6.4. Supplementary test and repeated test

In the two- and three-item test of General Examination or the Industry-Specific Examination (two-item test of Basic and Methods Knowledge and Practical Experience for grades I and II NDT qualifying test; three-item test of Basic Knowledge, Methods Knowledge and Practical Experience in the General Examination of grade III NDT qualification; and two-item test of Basic and Methods Knowledge and Practical Experience in grade III NDT qualifying examination), all marks are over 70 percent but the General Assessment mark is lower than 80 percent (not passed), the items with marks lower than 80 percent are allowed a supplementary test within a year. If the General Assessment mark is still lower than 80 percent after the supplementary test, all items should be repeatedly tested.

Those applying for a repeated test should file for the test according to the sequence of test applications.

If not approved in qualification for qualifying applicants, they can take part in a repeated test only after two months. If corruption and dishonesty are discovered in the qualifying test, such applicants can apply for a repeated test only after two years.

7. Certificate

7.1. Issuing of certificate

For those with a passing mark in the examination and with approved qualification evaluation, certificates are issued by the administrative department upon receiving a report from the Qualifying Body.

7.2. Form of certificate

Refer to Annex A (supplement) for the form of certificate, which was filled with details by the certificate issuing unit. At the right lower corner of the personal photograph of certificate holder, the certified NDT methods and grades of technical qualification are printed for the certificate holder along with stamped seal and signature of the responsible person of the Qualifying Body; certificate issuing date and effective period are also printed. For extension of effective date of the certificate, a special extension seal of the Qualifying Body should be stamped. Number should be filled on a certificate based on stipulations of file management.

7.3. When a certified NDT personnel is transferred from an industrial department to another, the second department should recognize the personnel's marks in the General Examination, and his general technical qualification.

8. Effective Period and Its Extended Effective Period of Certificate

8.1. Effective period

The effective period of a certificate is at most five years beginning from the issuing date.

In the following situations, the certificate should be revoked and cancelled:

a. The certificate holder is a person deprived of political rights.

b. The certificate holder made a major mistake in NDT specialty work.

c. The certificate holder left his unit of NDT work for more than a year.

8.2. Extension of effective period

At the end of an effective period, the Qualifying Body makes a recheck on the certificate holder. When the holder's provided proof is verified, another effective period of the certificate can be extended. Upon filing for extension of the effective period, the holder should provide the following proofs issued by the personal division of his work unit:

a. Proof of passed physical checkup; and

b. Proof that the certificate holder did not leave NDT work for more than a year.

9. Renewal Certification

9.1. At the end of the second extension period, the certificate holder should file with the Qualifying Body for a renewal certification. Upon approval of the renewal certification, the old certificate holder is issued a new extended period certificate. Those filing for renewal certification should provide the two above-mentioned proofs for extension of the effective period.

9.2. Renewal certification test

This is a simplified test approved by the Qualifying Body with the following contents:

a. For grades I and II NDT personnel, the operation test covers the general basic and the necessary industrial department according to the simplified stipulations.

b. For grade III personnel, a written test of applied technical knowledge is conducted with 20 test questions of general basic or of the necessary industrial department.

If the test mark is over 60 percent, the renewal certification is passed with issuing of a new effective date proof.

10. File

The Qualifying Body should maintain the following files:

10.1. A registration chart should be filed by the personnel to be certified according to different grades, different NDT methods and different departments for classification.

10.2. For the personal file of each personnel to be certified, and for each personnel whose certificate is revoked, the following contents should be included:

a. Test data: test questions the personnel answered, operation records and documents, written NDT process and technical manual, and test grade report card;

b. Proofs for extending the effective period and renewing certification; and

c. Other necessary materials that are required to maintain.

**ANNEX A: FORM OF TECHNICAL QUALIFICATION CERTIFICATE FOR NDT
PERSONNEL (SUPPLEMENT)**

A1. Composition of Qualifying Certificate

The qualification certificate is composed of three parts: jacket, cover and core. The cover and core is bound together with thread.

A2. Plastic Jacket

A2.1. Dimensions of the plastic jacket are 166x112 mm. The front surface is printed with golden letters; there are two pockets in the back of the jacket. Spacing of pocket openings is 26 mm (refer to Figs. A1 and A2).

A2.2. The material for the front surface of the plastic jacket is made of colored plastic fabric; selection of colors is as follows:

- a. Red for grade III certificate;
- b. Sky blue for grade II certificate; and
- c. Deep green for grade I certificate.

A2.3. Material for the pocket at back of the plastic jacket is of colorless, transparent plastic film.

A3. Cover

A3.1. Dimensions of the cover are 152x104 mm; the cover is made of soft lining paper (refer to Fig. A3).

A3.2. It is vacant without any letter of any color at the front surface (cover 1 and cover 4) of the cover; its back (cover 2 and cover 3) is white; printed on cover 3 are black letters and lines.

A4. The Core

A4.1. The core is composed of three sheets of high grade printing paper; dimensions of the paper are the same as that of the cover. There are altogether 12 sheets after binding.

A4.2. All letters and lines printed on each sheet of paper are black (refer to Figs. A4 to A9):

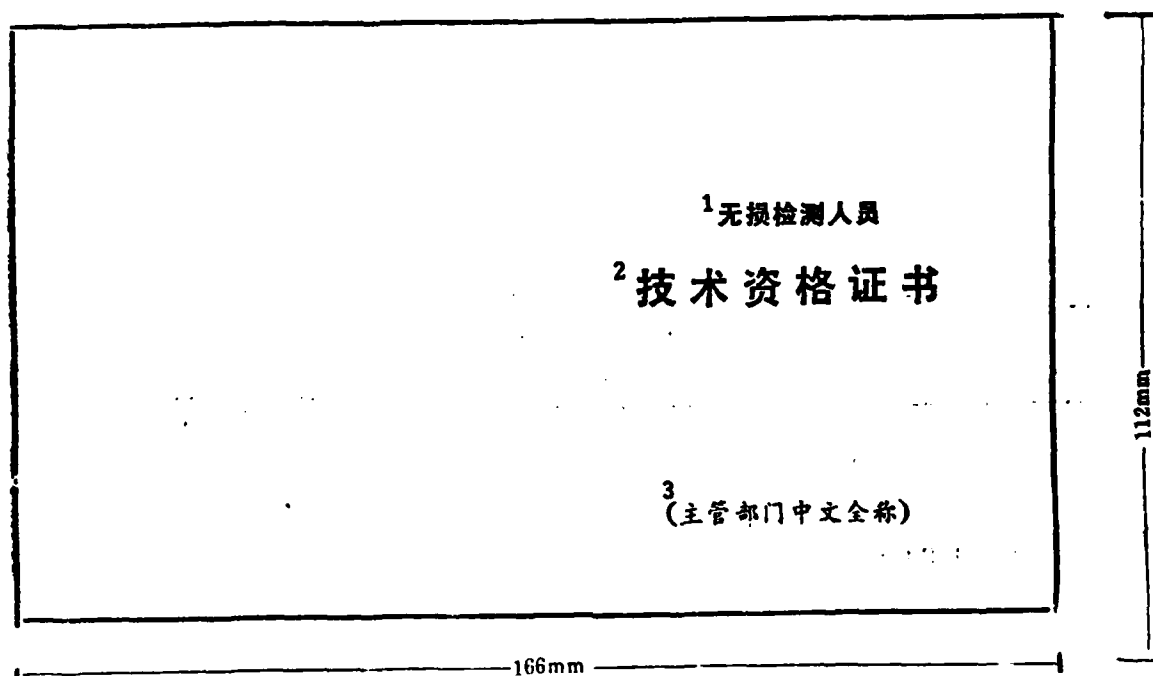


Fig. A1. Front surface of jacket
KEY: 1 - NDT personnel 2 - Technical
qualifying certificate 3 - Full name
in Chinese for the administrative
department

Footnotes:

1. This standard was proposed by the State Commission of Machinebuilding Industry.
2. This standard was drafted and filed by the Shanghai Institute of Material Science, State Commission of Machinebuilding Industry.

MODELS SD-I AND SD-IA IRIDIUM¹⁹² GAMMA-RAY FLAW DETECTING MACHINE

Iridium¹⁹² gamma-ray flaw detection machines are manufactured by this factory licensing an imported advanced technique from abroad. This kind of flaw detection machine was certified by the former Ministry of Hydroelectric Power; the manufacture of these machines is monitored by the Institute of Electric Power Construction of the Ministry of Energy.

Maximum capacities: for model I, iridium¹⁹², 60 curies; for model IA, iridium¹⁹², 100 curies;

exposure range: 10 to 100mm for steel products, and ± 300 mm for concrete;

focus of radiation source: outside diameter 2x2, outside diameter 2 x 3, outside diameter 3 x 3;

leakage dose: meets the international standard ISO 3999;

methods of transmitting radiation source: manual and automatic;

operating distance: 15 to 18mm;

length of radiation source output: 5 to 8m;

weight: 15kg for model I, and 20kg for model IA; and

dimensions of the vessel: for model I, 290x110mm; for model IA, 290x118mm.

The automatic control attachment has the functions of time delay start, automatic output of radiation source, exposure with timer, automatic return, and manual control in the case of malfunctioning or power loss, among other functions.

This factory applied the coordination of the machine radiation source and the radiation source changer for ensuring user demand by periodic supply of the radiation source. The following items of equipment are attached to the machine: dosage monitoring instrument, gamma-ray exposure calculating rule, and protective clothing. In addition, this factory provides the following services for users: on-site instruction, on-site maintenance and repair, as well as recovery of waste radiation source, among other services. Purchases are welcomed either with written letter or dispatching of purchasing agent to the plant.

In addition, this plant provides the following products to users:

SD143-85 single-wire exposure meter; SD143-85 defect depth measuring meter; SD143-85 slot depth measuring meter; GB5618-85 linear model quality meter; GB3323-87 equal-diameter image quality meter; GB3323-87 standard film evaluation rule; as well as GB3323-87 and SD143-85 film evaluation observation rule; film cementing frame; enhancement screen; protection plate; ordinary and multifunction dark boxes; and high-polymer lead equivalent protection plate.

Haimen Flaw Detection Consortium Plant, Institute of Electric Power Construction, Ministry of Energy

Plant site: Sanyang Town (chen), Haimen, Jiangsu; plant
superintendent: Xing Fei;

Telephone: Haimen 3644x59; Telegram: 4226

DISTRIBUTION LIST

DISTRIBUTION DIRECT TO RECIPIENT

<u>ORGANIZATION</u>	<u>MICROFICHE</u>
CS09 BALLISTIC RES LAB	1
CS10 R&T LABS/AVEADCOM	1
CS13 ARRADCOM	1
CS35 AVRADCOM/TSARCOM	1
CS39 TRASANA	1
Q591 FSTC	4
Q619 MSIC REDSTONE	1
Q008 NTIC	1
E053 HQ USAF/INET	1
E404 AEDC/DOF	1
E408 AFWL	1
E410 AD/IND	1
F429 SD/IND	1
P005 DOE/ISA/DDI	1
P050 CIA/OCR/ADD/SD	2
AFTT/LDE	1
NOIC/OIC-9	1
CCV	1
MIA/PHS	1
LLYL/CODE L-309	1
NSA/RSI-1	1
NSA/T513/TDL	2
ASD/FTD/TTIA	1
FSL	1